Mesoproterozoic Paleomagnetism of the Southern Congo Craton

Tierney E. Larson

Advisor: David A. D. Evans, Yale University
Second Reader: Richard E. Hanson, Texas Christian University

A Senior Thesis presented to the faculty of the Department of Geology and Geophysics, Yale University, in partial fulfillment of the Bachelor's Degree.

TABLE OF CONTENTS

ABSTRACT

The Congo-São Francisco (SF) craton is a keystone of Gondwana and also a possible part of the Precambrian supercontinent Rodinia, but its movement through Mesoproterozoic time still remains mostly unconstrained due to sparsity of reliable paleomagnetic data. Paleomagnetic results from 1.4 to 1.1 Ga igneous rocks from the southern Congo-SF craton help define a new apparent polar wander (APW) path for the craton. For this thesis project, we sampled Mesoproterozoic rocks from three different geological units in northern Namibia. The oldest of these is the Kunene Anorthosite Complex, dated at ~1370 Ma. In the southern Kunene area, the anorthosite complex is intruded by Epembe syenites (~1220 Ma) and related dolerite dykes, and in the eastern area near Swartbooisdrif, the anorthosite is intruded by both dolerite and carbonatite dykes (~1130 Ma). Our results include a positive baked-contact test for a Swartbooisdrif dyke intruding Kunene anorthosite, a positive conglomerate test in the Kunene region, and a pre- or syn-fold remanence from the anorthosite sampled around margins of the Zebra Mountains dome. The new, preliminary paleomagnetic poles are compared to those of similar ages from the Kalahari craton to evaluate alternative paleogeographic hypotheses for the two cratons prior to their Cambrian consolidation via the Damara orogeny. A fixist model, which places cratons in their present-day positions, is not supported by the pole comparisons. Alternative reconstructions that either optimize a joint 1.2-1.1 Ga apparent polar wander path for the two cratons, or produce a "closest-approach" juxtaposition based on the same data, are considered unlikely based on their plate-kinematic or tectonostratigraphic implications. In a final integrative solution of all three pairs of poles, we rotate the Kalahari craton to the southeast of the Congo-SF craton in what could have been a long-lived connection, exploiting the relation between Umkondo magmatism and coeval dykes extending into the Congo-SF craton.

INTRODUCTION

Constraining the motion of continents throughout Precambrian time is an essential first step in understanding large-scale tectonic processes and the possible cyclicity of supercontinents. Using paleomagnetism, a more complete understanding of Earth's geomagnetic field through history can be obtained, and proposed continental reconstructions can be tested. To better define the breakup of the supercontinent Nuna and the subsequent assembly of Rodinia, paleomagnetic studies of Mesoproterozoic rocks are essential. The Congo-São Francisco craton is ideal for this analysis not only due to its vast size (comprising both modern day central Africa and eastern Brazil), but also because the craton was paleogeographically central to Gondwana and Pangea (Figure 1). Likely a major constituent of both Nuna and Rodinia (Ernst et al., 2013; Evans et al., 2015), the Congo- São Francisco (SF) craton is an important component of Precambrian continental reconstructions.

Rocks from 1.4 to 1.1 Ga were sampled in northernmost Namibia, within the Congo-SF craton, in order to enhance its sparse Mesoproterozoic paleomagnetic record. Three igneous suites are investigated: the ~1370 Ma Kunene Anorthosite Complex, the ~1215 Ma Epembe syenites and related dolerite dykes, and the ~1130 Ma Swartbooisdrif carbonatite/syenite dykes. Through thermal demagnetization, statistical analysis, and implementation of field stability tests, this sizeable set of nearly 400 samples is expected to yield high-quality paleomagnetic poles, contributing to a more robust reconstruction of Precambrian Congo-SF movement. The only previously published paleomagnetic work dealing with late-Mesoproterozoic rocks from this area was done by Piper in 1974, in his reconnaissance study of the Kunene anorthosite in Angola. Results found here are compared and contrasted with Piper's for a more complete understanding of the unit. More locally, determining the position of Congo-SF in the Mesoproterozoic would allow for a comparison with the location of the Kalahari craton at the same time, helping to provide further insight into the characteristics of a former ocean between the two cratons, as well as the subsequent collisional orogeny of the Damara belt through central Namibia (Prave, 1996; Grunow et al. 1996; Gray et al., 2006).

REGIONAL GEOLOGY

Three separate units near the Angola-Namibia border were sampled during the 2014 austral winter field season: the Kunene Anorthosite Complex, the Swartbooisdrif dolerite and carbonatite dykes, and the Epembe syenites and related doleritic dykes. The largest of these three units is the Kunene Anorthosite Complex (Figure 2), which spans nearly 18,000 square kilometers and consists mainly of massive white anorthosite intruded by dark leucotroctolite (Maier et al., 2013). Dark leucotroctolite intrusions have been dated, using U-Pb in baddeleyite, at 1363±17 Ma (Maier et al., 2013). At the southern edge of the complex, the Zebra Mountain lobe of interlayered dark leucotroctolite and white anorthosite is the most prominent feature and has been dated using a U-Pb zircon age from a leucogabbronorite at 1385±25 Ma (Drüppel et al., 2000). The satellite mafic and ultramafic intrusions and numerous troctolitic sills within the anorthosite suggest sequential mantle upwellings along the southern boundary of the Congo-SF craton during the Mesoproterozoic (Maier et al., 2013). The 19 sites sampled for the Kunene component of this project are located along the western and southern boundaries of the lobe, comprising 11 sites of light and dark anorthosite, four sites of mafic or ultramafic periphery rocks, two sites of syenite intrusions, and one conglomerate test.

Swartbooisdrif, a region on the southeastern margin of the Kunene complex, is an area characterized by pervasive swarms of syenite, nepheline syenite, and ferrocarbonatitic dykes (Drüppel et al., 2005). Thirteen sites were sampled from this region, including six sites of doleritic or generally mafic dykes, three sites of feldspathic dykes and anorthosite, and four sites of carbonatitic dykes (Figure 3). Just outside the small settlement of Swartbooisdrift, the Kunene complex is cut by numerous SE- and ENE-trending shear zones (Drüppel et al., 2005) leading to the intrusion of these dykes, occasionally outcropping as sodalite-bearing metasomatites hosted in carbonatite (von Seckendorff et al., 2000). The ferrocarbonatitic dykes are thought to be 1120-1140 Ma (Littmann et al., 2000) and are host to considerable amounts of sodalite.

Completing this series of southern Congo craton rocks is the Epembe alkaline suite, which is located near the southern flanks of the Zebra Mountains (Figure 4). This complex area is characterized by a nepheline syenite plug surrounded by carbonatite and lamprophyric dykes which intrude the gneisses of the Epupa Metamorphic Complex (Ferguson et al., 1975; Miller, 2008). Layered, glomerophyric, and plutonic nepheline syenites are intruded sporadically by carbonatite and dolerite dykes. These syenites, situated along WNW-trending faults (Miller, 2008), appear in many forms, including both fine- and coarse-grained, porphyritic, banded, foliated, layered,

brecciated, and pegmatitic (Ferguson et al., 1975; Menge, 1986, 1996). Concordant U-Pb ages from zircons for two samples of nepheline syenite of 1216±2.4 Ma and 1213±2.5 Ma have been reported (Seth et al., 2003). The seven sites in this locality are evenly distributed across the region, with three sites sampling syenites, three sampling mafic (doleritic or generally mafic) dykes, and one site (L14E02) made up of amphibolite basement rocks.

Site locations and field descriptions are listed in Table 1. Site mean characteristic remanent magnetization directions are listed in Table 2.

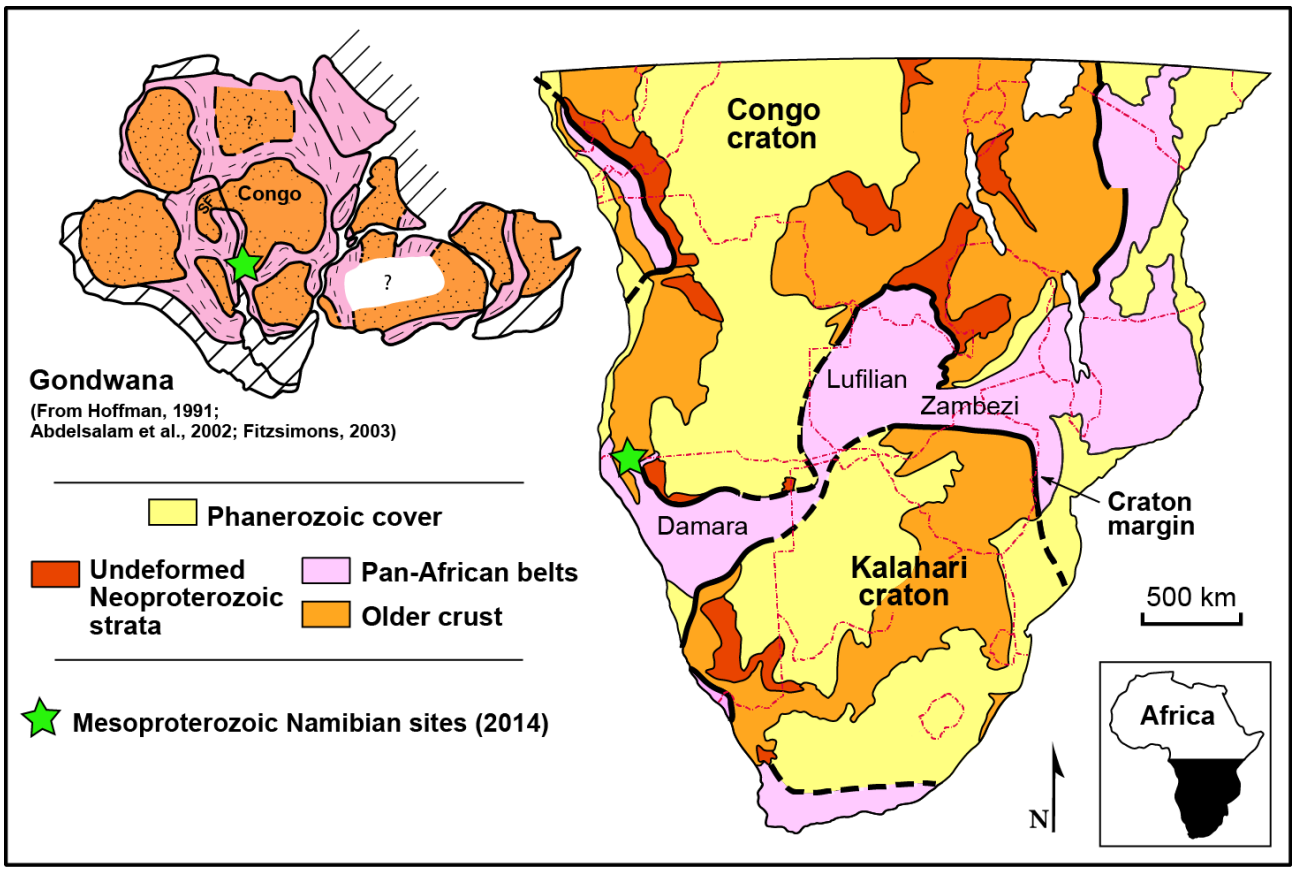

Figure 1: Southern Africa is made up of the Kalahari and the Congo cratons, sutured together by Pan-African orogenic belts: the Damara, Lufilian, and Zambezi. The study area (marked by a star) is in the southwestern Congo craton, which, combined with the São Francisco (SF) craton in Brazil, is considered the centerpiece of Gondwana. Adapted from Hanson (2003).

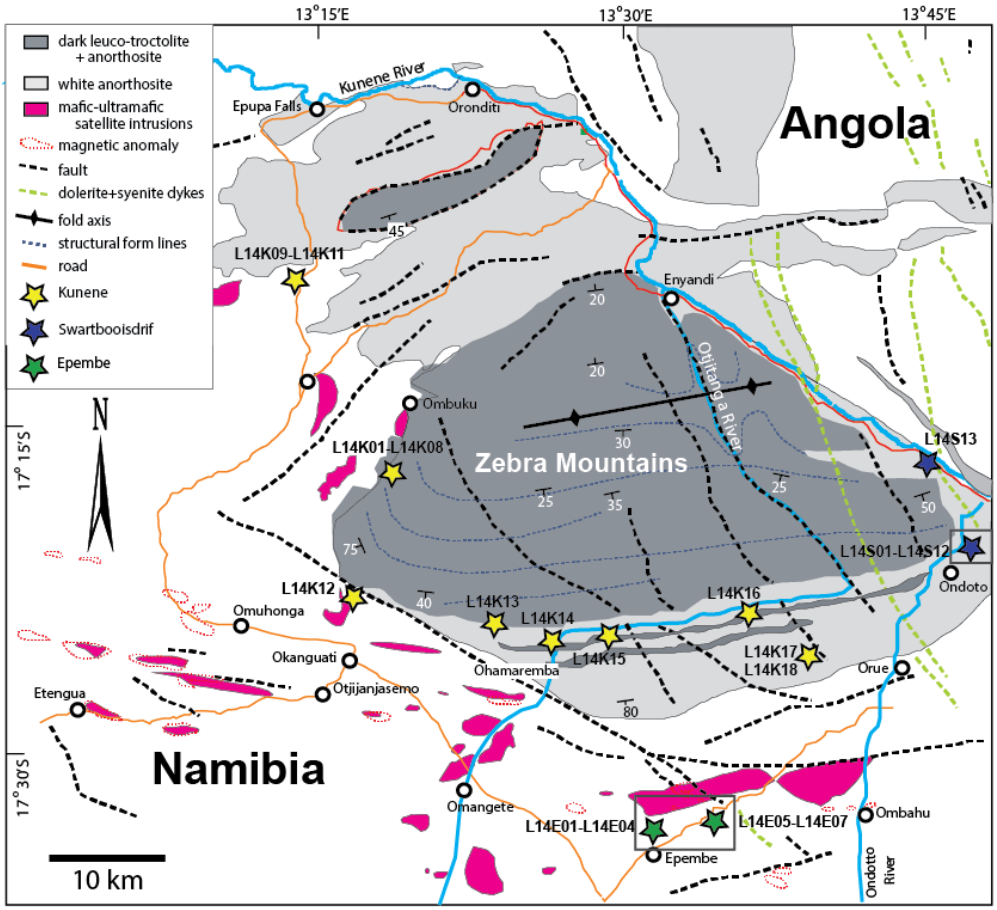

Figure 2: The Kunene Anorthosite complex spans the Namibia-Angola border and is centered on the Zebra Mountain Lobe. Sampling sites (marked by stars) are located in three main areas around the mountains: the Kunene complex (yellow), Epembe (green), and Swartbooisdrif (blue). Gray boxes around the Epembe and Swartbooisdrif areas denote insets of more detailed maps included as the next two figures. Adapted from Maier et al. (2013).

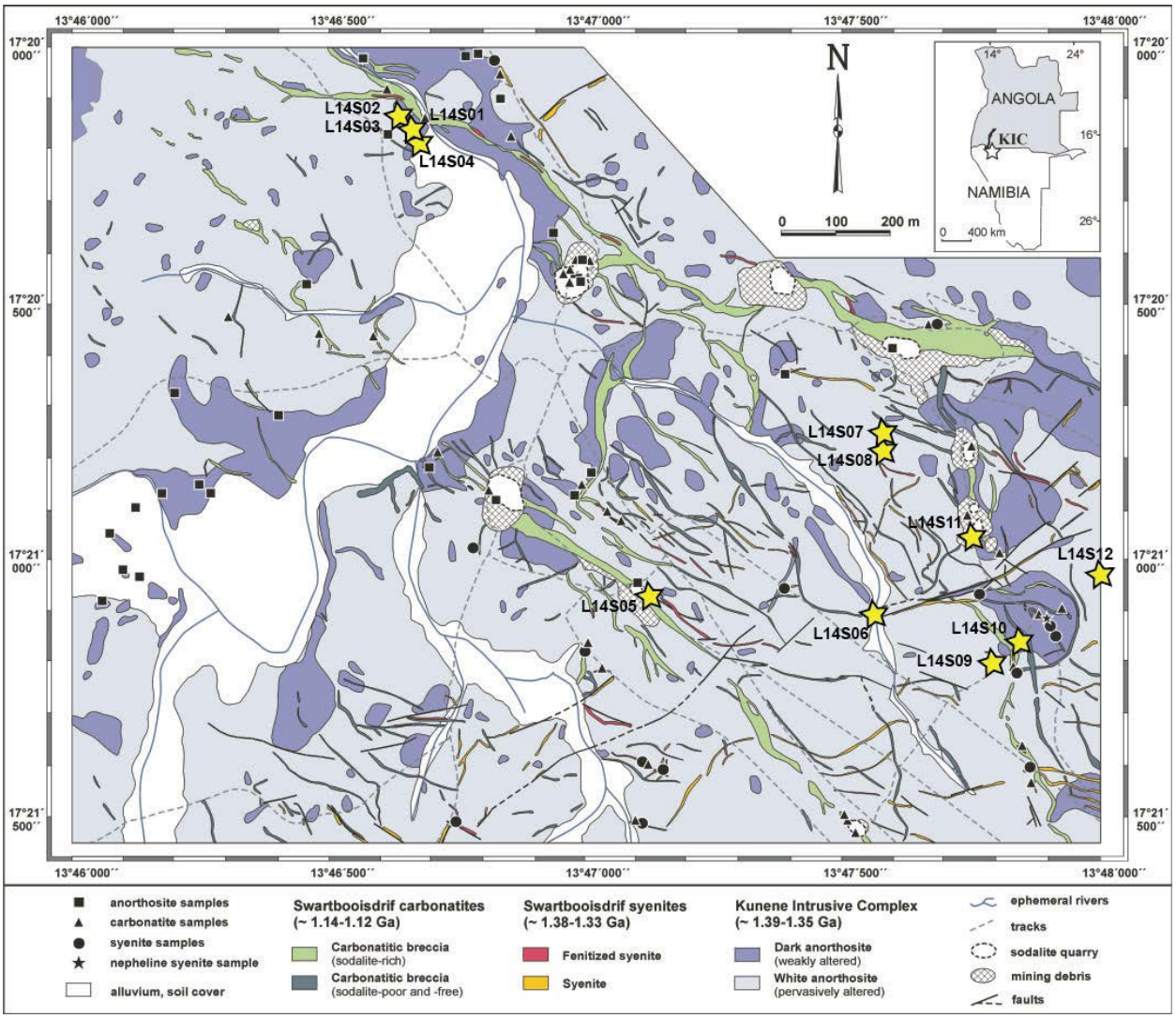

Figure 3: Dyke swarms transect the southeastern margin of the Kunene Intrusive Complex (KIC), making up the Swartbooisdrif region of carbonatites and syenites. Sample sites are shown as yellow stars. Adapted from Drüppel et al. (2005)

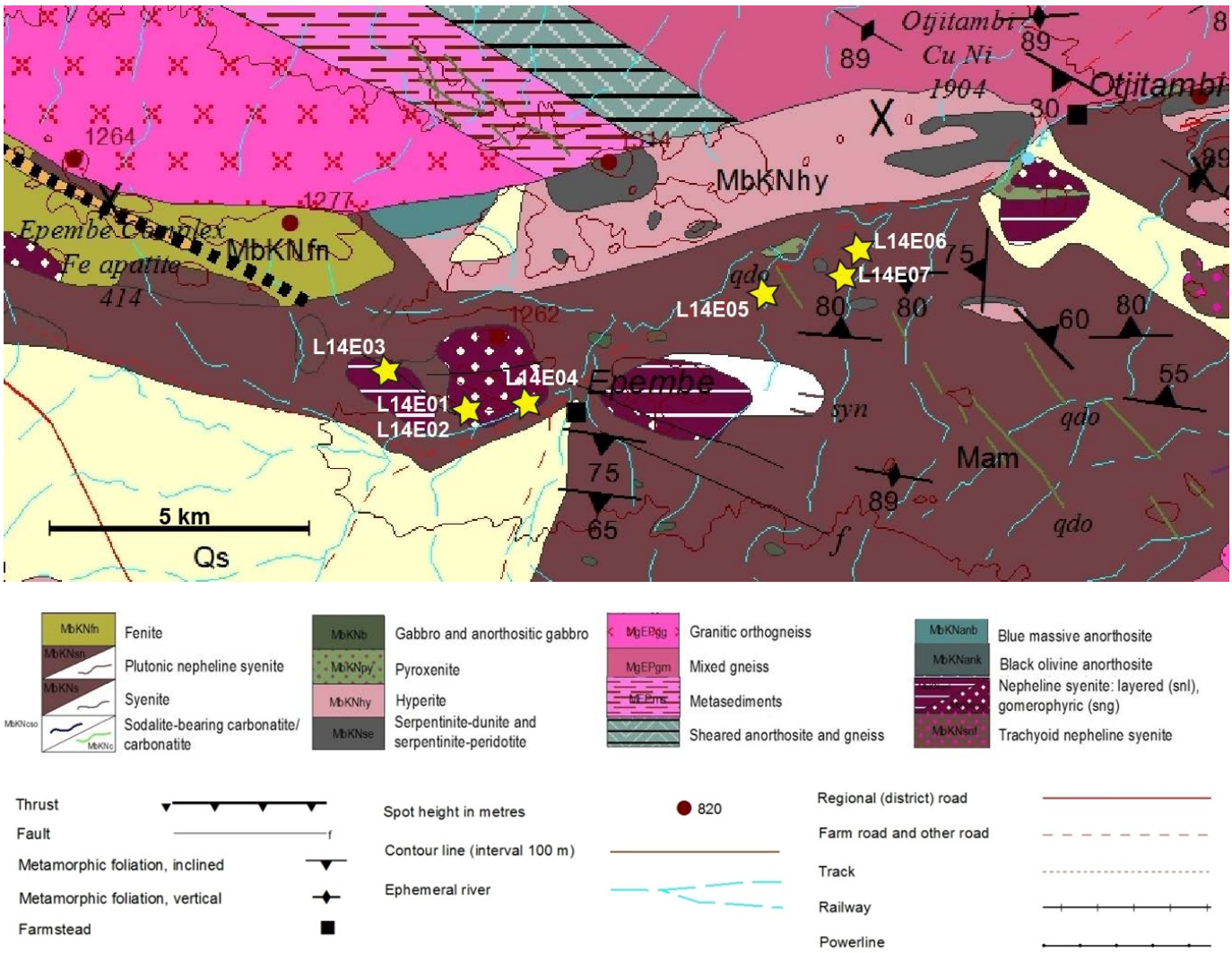

Figure 4: The Epembe region is largely made up of a syenite plug which intrudes the gneisses of the Epupa Metamorphic Complex. Sample sites are shown as yellow stars, and sites L14E05-L14E07 are from northwest-southeast trending dolerite dykes. Adapted from Schreiber (2002).

Table 1. Paleomagnetic site information for this study.
Kunene Anorthosite Complex

NAME	LOCATION	N	LAYERING RHS°/DIP°	LITHOLOGY	EXTRA INFO
L14K01	17.27785°S 13.32081°E	8	--	Syenite dyke intruding anorthosite	
L14K02	17.27785°S 13.32081°E	10	179.8 / 71	Coarse anorthosite intruded by K01	All samples near dyke margin
L14K03	17.27795°S 13.32105°E	8	184.1 / 71	Layered dark syenite and light anorthosite	
L14K04	17.27787°S 13.32106°E	9	185.8 / 49	Dark syenite	
L14K05	17.27787°S 13.32106°E	9	187.0 / 49	Light anorthosite	
L14K06	17.27787°S 13.32106°E	9	178.2 / 69	Dark anorthosite	
L14K07	17.27614°S 13.31776°E	8	174.5 / 54	Pyroxene pegmatite	
L14K08	17.27539°S 13.31680°E	7	161.1 / 40	Dark anorthosite	
L14K09	17.13930°S 13.23717°E	9	215.8 / 46	Anorthosite with mafic layers	
L14K10	17.13931°S 13.23698°E	8	165.0 / 42	Dark anorthosite	
L14K11	17.13981°S 13.23659°E	8	163.8 / 44	Dark anorthosite	
L14K12F	17.38627°S 13.28196°E	10	262.7 / 04	Felsic cobbles in conglomerate	Conglomerate test
L14K12M	17.38627°S 13.28196°E	15	262.7 / 04	Mafic cobbles in conglomerate	Conglomerate test
L14K13	17.40864°S 13.39814°E	8	074.3 / 44	Altered dark anorthosite	A+B = darker phase; C+D = lighter phase; E+F = plag. + opx; G+H = altered
L14K14	17.41927°S 13.44328°E	8	093.8 / 50	Dark anorthosite	
L14K15	17.41577°S 13.48484°E	8	062.8 / 38	Dark, mafic, weathered rock	Two separate units ~20m apart (A-D and E-H)
L14K16	17.39488°S 13.60256°E	8	085.6 / 48	Dark anorthosite	

L14K17	17.42818°S 13.65169°E	7	085.1 / 48	Dark anorthosite	Magnetized in some areas
L14K18	17.42895°S 13.65190°E	8	055.8 / 63	Dark mafic rock	
L14S04	17.33579°S 13.77751°E	6	046.0 / 55	Unaltered anorthosite	Part of Kunene Complex

Swartbooisdrif Dykes

NAME	LOCATION	N	LAYERING RHS°/DIP°	LITHOLOGY	EXTRA INFO
L14S01	17.33550°S 13.77745°E	9	--	Feldspar with hematite inclusions	
L14S02	17.33529°S 13.77741°E	7	--	Fine-grained carbonatite	Pyrite veins in G; A, B, C drilled into host rock
L14S03	17.33529°S 13.77741°E	7	046.0 / 55	Mottled anorthosite intruded by S02	A contains some carbonatite
L14S05	17.35108°S 13.78495°E	9	--	Weathered carbonatite dyke	A-E = fine-grained; F-I = coarse-grained
L14S06	17.35179°S 13.79238°E	9	--	Weathered mafic dyke	
L14S07	17.34584°S 13.79239°E	9	--	Weathered mafic dyke	Very broken up; lots of boulders
L14S08	17.34619°S 13.79234°E	12	--	Coarse dolerite	G-L from second outcrop ~25m from A-F
L14S09	17.35309°S 13.79634°E	8	--	Dark mafic dyke	Slightly magnetized
L14S10	17.35250°S 13.79722°E	9	--	Intermediate dyke	
L14S11	17.34906°S 13.79562°E	9	--	Brown weathered carbonatite	
L14S12	17.35029°S 13.80096°E	8	--	Dark mafic dyke	
L14S13	17.27848°S 13.74743°E	10	--	Dolerite dyke	A-F ~3m below G-J

Epembe Syenites and Dolerites

NAME	LOCATION	N	LAYERING RHS°/DIP°	LITHOLOGY	EXTRA INFO
L14E01	17.57482°S 13.52117°E	7	--	Glomerophyric nepheline syenite	Epidote coats nepheline syenite apophyses
L14E02	17.57482°S 13.52117°E	5	--	Amphibolite basement rock	Very friable
L14E03	17.56955°S 13.50914°E	7	--	Layered nepheline syenite	A-D = medium-grained; E-G = coarse-grained
L14E04	17.57286°S 13.53030°E	7	--	Nepheline syenite	
L14E05	17.55524°S 13.57151°E	7	--	Dolerite dyke	Magnetized in some areas
L14E06	17.55206°S 13.58556°E	7	--	Dark gray-green dyke	A, B = coarse-grained; C-G = finer-grained
L14E07	17.55484°S 13.58333°E	8	--	Dolerite dyke	E and F furthest from contact

Notes: N, number of oriented core samples collected. RHS, Right-hand strike. In the rightmost column, letters refer to names of specific samples.

Table 2. Site mean characteristic remanent magnetization (ChRM) directions
Kunene Anorthosite Complex

NAME	LITHOLOGY	n/N	Geog. Dec°	Geog. Inc°	75%TC Dec°	75%TC Inc°	100%TC Dec°	100%TC Inc°	k	a95°	VGP Lat°N	VGP Long°E
L14K01	Syenite dyke intruding anorthosite	6/8	239.9	-12.8	N.A.	N.A.	189.1	-57.3	36.5	22.7	-34.1	202.0
L14K02	Coarse anorthosite intruded by K01	9/10	228.3	-52.4	N.A.	N.A.	303.8	43.6	36.5	25.8	20.6	-040.0
L14K03	Layered dark syenite and light anorthosite	N.A.	No	Group	mean	apparent	at this	site	N.A.	N.A.	N.A.	N.A.
L14K04	Dark syenite	7/9	302.7	51.9	N.A.	N.A.	292.1	5.8	36.5	17.3	20.1	-066.7
L14K05	Light anorthosite	6/9	320.6	54.7	N.A.	N.A.	301.1	12.6	36.5	15.1	27.2	-59.8
*L14K06	Dark anorthosite	5/9	272.6	-21.4	282.1	-72.7	184.2	85.9	36.5	43.8	-25.4	12.6
*L14K07	Pyroxene pegmatite	4/8	279.6	-27.9	298.2	-65.5	326.5	-74.9	36.5	28.4	39.8	213.2
L14K08	Dark anorthosite	3/7	211.4	68.0	N.A.	N.A.	234.7	31.7	36.5	45.5	-37.9	-068.1
L14K09	Anorthosite with mafic layers	6/9	287.7	-64.9	N.A.	N.A.	325.3	66.8	36.5	10	16.7	-009.6
L14K10	Dark anorthosite	6/8	240.7	-64.4	N.A.	N.A.	275.1	71.9	36.5	39.2	-11.5	-020.6
L14K11	Dark anorthosite	5/8	239.2	67.4	N.A.	N.A.	247.7	23.9	36.5	22	-24.7	-070.6
L14K12F	Felsic cobbles in conglomerate test	N.A.	No	Group	mean	apparent	at this	Site	N.A.	N.A.	N.A.	N.A.
L14K12M	Mafic cobbles in conglomerate test	N.A.	No	Group	mean	apparent	at this	Site	N.A.	N.A.	N.A.	N.A.
*L14K13	Variably altered dark anorthosite	6/8	187.7	-81.4	336.3	-64.7	338.5	-53.7	36.5	12.5	54.8	222.1
*L14K14	Dark anorthosite	8/8	264.6	-69.3	330.2	-50.9	336.7	-40.1	36.5	5.2	59.5	250
L14K15	Weathered mafic rock, two outcrops ~20m apart	4/8	358.3	-45.0	N.A.	N.A.	350.7	-09.5	36.5	24.4	74.4	-023.4
L14K16	Dark anorthosite	7/8	356.6	-37.1	N.A.	N.A.	353.2	6.2	36.5	15.3	68.4	-005.2
L14K17	Dark anorthosite, slightly magnetic	5/7	292.3	10.3	N.A.	N.A.	275.9	27	36.5	23.6	01.2	-060.9
L14K18	Dark mafic rock	7/8	222.8	-11.3	N.A.	N.A.	240.3	-16.6	36.5	23.9	-25.1	265.2
*L14S04	Unaltered anorthosite	3/6	317.8	60.5	311.7	-78.2	314	-64.6	36.5	25	31.3	213.4

Swartbooisdrif Dykes

NAME	LITHOLOGY	n/N	Geog. Dec°	Geog. Inc°	75%TC Dec°	75%TC Inc°	100% TC Dec°	100% TC Inc°	k	a95°	VGP Lat°N	VGP Long° E
L14S01	Feldspar-rich with hematite inclusions	N.A.	No	group	mean	apparent	at this	site	N.A.	N.A.	N.A.	N.A.
*L14S02	Fine-grained carbonatite	6/7	264.9	30.4	N.A.	N.A.	N.A.	N.A.	8.07	13.6	-09.5	-062.0
*L14S03	Coarse anorthosite intruded by S02	4/7	257.2	31.0	N.A.	N.A.	N.A.	N.A.	8.07	12.4	-16.7	-063.5
L14S05	Weathered carbonatite dyke, variable grain size	7/9	199.3	53.8	N.A.	N.A.	N.A.	N.A.	8.07	13.9	-65.8	-028.0
L14S06	Weathered mafic dyke	6/9	323.9	-44.0	N.A.	N.A.	N.A.	N.A.	8.07	30	55.5	263.2
L14S07	Weathered mafic dyke	7/9	201.8	28.6	N.A.	N.A.	N.A.	N.A.	8.07	19.5	-69.0	281.3
*L14S08	Coarse dolerite, two outcrops ~25m apart	6/12	222.9	-01.6	N.A.	N.A.	N.A.	N.A.	8.07	7	-44.0	265.0
L14S09	Dark mafic dyke, slightly magnetic	4/8	358.6	11.0	N.A.	N.A.	N.A.	N.A.	8.07	24.5	67.1	010.2
*L14S10	Intermediate dyke	7/9	255.4	-15.5	N.A.	N.A.	N.A.	N.A.	8.07	20	-11.4	271.7
L14S11	Brown weathered carbonatite	4/9	307.3	37.3	N.A.	N.A.	N.A.	N.A.	8.07	18.2	25.8	-041.8
*L14S12	Dark mafic dyke	5/8	249.9	-27.2	N.A.	N.A.	N.A.	N.A.	8.07	23.1	-14.1	263.4
*L14S13	Dolerite dyke	7/10	236.1	-11.6	N.A.	N.A.	N.A.	N.A.	8.07	10	-30.0	266.1

Epembe Syenites

NAME	LITHOLOGY	n/N	Geog. Dec°	Geog. Inc°	75%TC Dec°	75%TC Inc°	100% TC Dec°	100% TC Inc°	k	a95°	VGP Lat°N	VGP Long° E
*L14E01	Glomerophyric nepheline syenite with epidote	5/7	226.4	-31.1	N.A.	N.A.	N.A.	N.A.	19	17.9	-32.9	248.1
L14E02	Amphibolite basement rock, very friable	0/5	No	group	mean	apparent	at this	site	N.A.	N.A.	N.A.	N.A.
L14E03	Layered nepheline syenite	4/7	349.9	55.9	N.A.	N.A.	N.A.	N.A.	19	10.9	35.2	003.6
L14E04	Nepheline syenite	7/7	282.9	45.4	N.A.	N.A.	N.A.	N.A.	19	36.1	03.1	-047.0
*L14E05	Dark mafic rock, slightly magnetic	6/7	244.1	-33.0	N.A.	N.A.	N.A.	N.A.	19	13.8	-17.7	257.4
*L14E06	Dark greenish mafic rock	6/7	271.7	-34.4	N.A.	N.A.	N.A.	N.A.	19	9.9	07.1	265.9
*L14E07	Dolerite dyke	8/8	221.8	-36.9	N.A.	N.A.	N.A.	N.A.	19	6.1	-34.1	242.4

Note: All sites marked with an asterisk (*) were included in the calculations of preliminary paleopoles for each unit.

METHODS

All 38 Namibian sites, from which a total of 319 oriented samples were collected, were scouted and sampled during a four-week field season in July, 2014. Sites were first identified on published geological maps (Schreiber, 2002) and Google Earth satellite imagery, and further field reconnaissance was done to find suitable outcrops for paleomagnetic sampling. At each site, seven to twelve samples were extracted using a portable rock drill with diamond-tip bit (examples of each rock type are shown in Figure 5). These cores, each 5-10 centimeters in length, were oriented *in situ* using an orientation device with solar and magnetic compasses and a clinometer (Figure 6). Most sites sampled a single rock type, but in some localities samples were taken from either side of an igneous margin in order to perform baked contact tests (L14K01/L14K02 and L14S02/L14S03). One large site with 26 total samples from both mafic and felsic clasts within a single unit (L14K12M and L14K12F) was collected in order to perform a conglomerate test. For sites where bedding or igneous layering was visible, strike and dip was measured to be later used as a paleohorizontal reference for tilt correction.

Samples were then taken back to Kline Geology Laboratory, Yale University, to be prepared for paleomagnetic analysis. Using a diamond-bladed rock saw, cylindrical samples around 2.5 centimeters in diameter and one to two centimeters in height were trimmed from each core. The samples were sanded (if needed) and individually labeled, and computer files containing location, description, and orientation of each sample were created using field notes. In the Yale Paleomagnetic Facility, the samples were analyzed using a cryogenic DC-SQuID magnetometer with automated sample changer. Initial natural remanent magnetization (NRM) measurements were recorded, then samples (separated into five groups for constant rotation between demagnetization and remanence acquisition) were immersed in liquid nitrogen and measured again. Each following successive step included thermal demagnetization, where samples were placed in magnetically shielded ovens, heated to increasingly higher temperatures, and held at peak temperatures for around ten minutes. Temperature increases got smaller approaching Curie temperatures (580°C for magnetite, 675°C for hematite), and samples remained in this cycle until completely demagnetized.

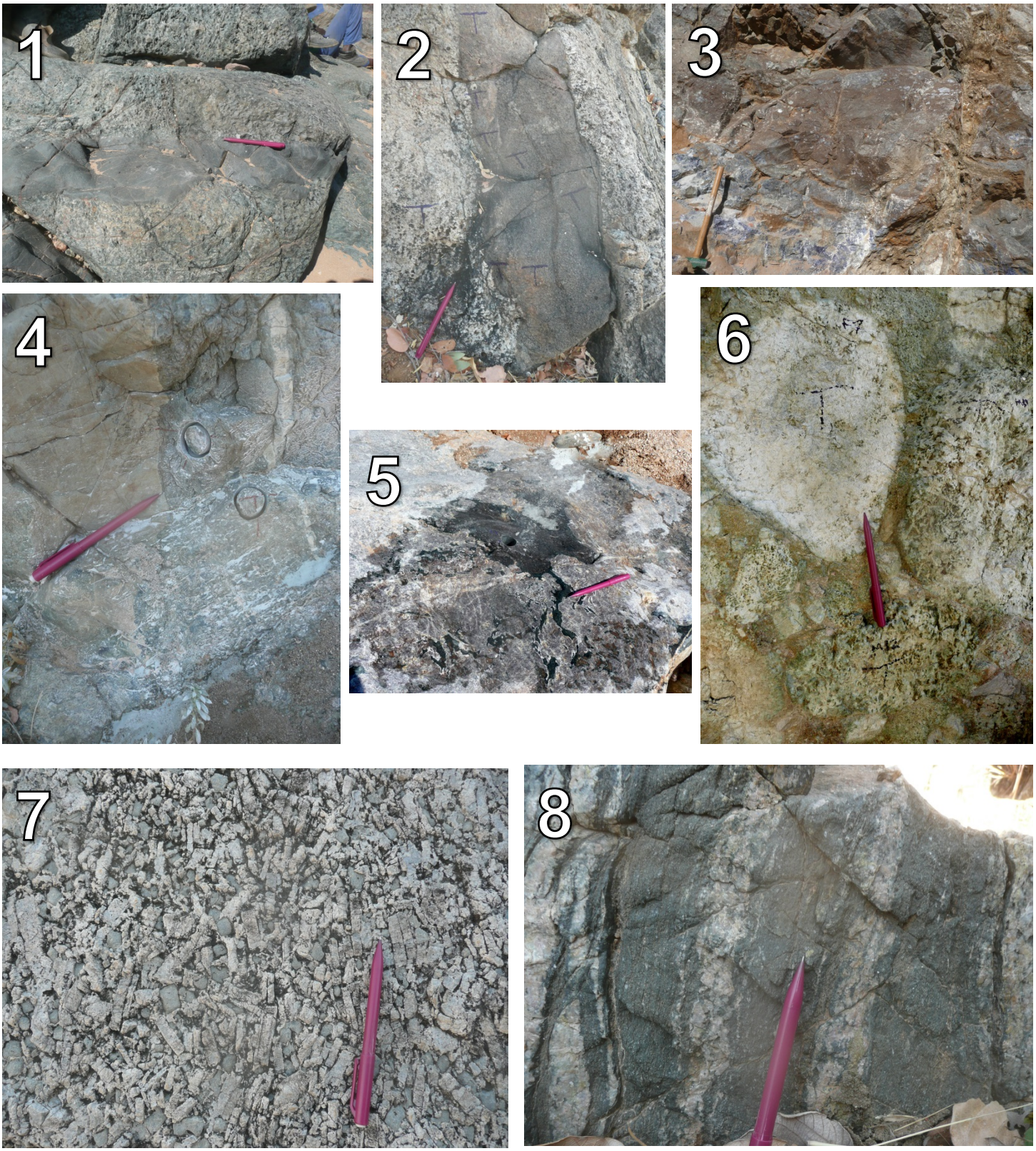

Figure 5: Typical field lithologies: 1) Baked contact between L14S02 and L14S03, 2) Intermediate dyke from L14S10, 3) Massive weathered carbonatite in abandoned sodalite quarry at L14S11, 4) Coarse anorthosite (L14K02, right) cut by syenite dyke (L14K01, left), 5) Anorthosite with weak mafic layering at L14K09, 6) Conglomerate test with felsic (L14K12F) and mafic (L14K12M) cobbles, 7) Coarse-grained nepheline syenite at L14E03, 8) Veins of nepheline syenite (L14E01) intruding basement amphibolite (L14E02). Pencil for scale except the ~1m-long sledgehammer in 3).

Figure 6: Components of sampling during the 2014 field season in Namibia: 1) Taking bedding measurements (can be done before or after drilling), 2) Drilling cores after marking sample locations, 3) Orienting cores, 4) Removing, labelling, and wrapping cores, 5) Inventory of field equipment carried to each site.

RESULTS AND INTERPRETATION

After thermally demagnetizing all samples, least squares analysis (Kirschvink, 1980; Jones, 2002) was done to fit lines and planes to each magnetic component revealed in orthographic projections. Components were labeled using a system of abbreviations including LOW (low-stability component, usually removed at the liquid-nitrogen step), LTH (low thermal, usually removed entirely below ~300°C, not decaying directly toward the origin), MTH (mid-thermal, usually removed by ~400-580°C, not decaying toward the origin), HTH (high thermal, persisting above ~580°C, but also not decaying toward the origin), MTO (magnetite-to-origin, a series of steps with constant direction, decreasing in magnitude through the ~500-580°C range), HTO (hematite-to-origin, as above but persisting to ~675°C), DTO (decay-to-origin, as above but crossing a wide range of unblocking temperatures), SEP (stable endpoint, the final few stable steps in a single direction and magnitude, prior to acquisition of spurious laboratory-induced magnetizations), and HPL (high plane, the plane containing any of the LTH, MTH, or HTH free lines, plus the origin). Wherever a component contained the origin as a datum (MTO, HTO, DTO, SEP, HPL), that component's fit was "forced" through the origin in the PaleoMag software code (Jones, 2002). After fits were made for each sample, the characteristic remanence direction was identified as a single data point plotted on an equal area projection of the unit sphere (Butler, 1992). For each site, these data points were analyzed with Fisher (1953) statistics to determine common component directions that agree with each other, and these were combined to calculate final Kunene, Swartbooisdrif, and Epembe mean directions. Paleomagnetic poles were created for each unit, which were then added to an animated continental reconstruction created with the program GPlates (Williams et al., 2012). Zijderveld and equal-area plots for selected sites representative of each unit are shown in Figures 7-17. All least-squares analyses can be found in the Appendix.

Kunene Anorthosite Complex

Nineteen sites were sampled from the Kunene Complex (including site L14S04, which is also Kunene anorthosite), but one was used purely for a conglomerate test. Of the other 18, seven were used in the calculation of a paleomagnetic pole. Least-squares fits were made for all sites, in both geographic and tilt-corrected reference frames. Summary data plots for the Kunene sites with meaningful results are shown in figures 7-13.

K01: This site contains eight samples taken from an east/west-trending, apparently vertical, riverbed syenite dyke which may or may not be consanguineous with the Kunene Complex. The dyke shows chilled margins against coarse anorthosite, which implies intrusion of the dyke into

surrounding Kunene anorthosite (~1370 Ma). For a baked contact test, samples are taken both near the margin and spaced further away. K02 samples the coarse anorthosite in immediate contact with the dyke, while K03 samples anorthosite at increasing distances from the dyke. In site K01, four of the samples begin with relatively weak magnetic moments on the order of 1e-05 or 1e-06 emu (C, D, G, H), while the other four have moderate moments all around 1e-03 emu. The weaker samples have messier orthographic plots that make fitting high-temperature components more difficult, so high planes were fit to all of these. All samples had a low-stability component, and most of these are clustered in a west-northwesterly shallow downward direction in geographic coordinates. The two major outliers to this cluster are sample A, which is geographically southwesterly shallow downward, and sample H, which is geographically northerly steep upward.

Only samples E and F had high-stability components fit with MTO lines, both of which give geographic directions in a north-northwesterly steep downward direction. The rest of the samples' high-stability components were fit with SEP lines and also HPL arcs in cases where no direct decay to the origin was discernible. Again, most of the component directions are northwesterly and downward, however they range from shallow to steep and do not form a well-defined cluster. With a tilt correction, most components are in an upward direction, but sweep from northwest to southwest, so they also do not for a well-defined cluster. Sample A is a major outlier again, with a geographically southwesterly shallow upward direction, and the second outlier is sample B in a geographically southwesterly shallow downward direction. Most planes suggest directions similar to sample A.

INTERPRETATION: The low-stability component from this site has a mean northwestern downward direction in geographic coordinates, and the high-stability component has a southwestern upward direction in geographic coordinates (Figure 7); the low-stability component is likely an overprint (Figure 9), of possible Pan-African age based on its similarity to Early Cambrian expected directions according to the Gondwana apparent polar wander path (Mitchell et al., 2010). The high-stability component may be primary, and, if so, could suggest a 1.2-1.1 Ga age for the dyke, based in comparison of the *in situ* direction with those from Epembe and Swartbooisdrif (see below). However, Fisher statistics have substantial error (a95 = 18.2° for low components and 27° for high components), and the dyke remains undated.

K02: Ten samples were taken from the coarse anorthosite in immediate contact with the syenite dyke of site K01. Distance from each sample to the dyke margin was recorded—the closest samples B, G, H, and J are all within two centimeters of the boundary, while the farthest are A and

D at ~11 and ~23 centimeters away, respectively. All samples begin with weak magnetic moments around 1e-05 or 1e-06 emu. Because of this, decay to the origin was difficult to discern, and measurements were mostly scattered in orthographic view. Low-stability components were not fit for samples C, E, and G, but the rest that were fit do not yield a consistent direction (five of seven are upward, but dispersed in all directions). The high-stability components do yield a consistent direction, however, using both stable endpoints and planes. Neither a low- nor a high-stability component could be fit for sample E, but seven of the remaining nine samples cluster generally in the south-southwesterly moderate upward direction, which tilt corrects to a southeasterly shallow upward direction. Using HPL instead of SEP fits gives the same general direction (both geographic and tilt-corrected) but with better Fisher statistics, so either set of principal component analyses can be used toward a site mean (Figure 7).

INTERPRETATION: These samples are all weakly magnetic, and some maintain a low-component direction similar to the one in L14K01 (Figure 9). However, the high-stability components were fit with SEP lines and HPL arcs, both of which provide a consistent geographic south-southwesterly mid-inclination upward direction (Figure 7). With a tilt correction this direction is southeasterly shallow upward. The high components are broadly similar to those from the dyke site K01, which suggests that the magnetic direction of the anorthosite is possibly an overprint from heating during intrusion.

K03: This site contains samples of the same layered dark and light, coarse anorthosite from sites K02, but these eight samples are taken at increasing distances from the K01 dyke. All samples begin with moderate magnetic moments (on the order of 1e-04 or 1e-05 emu), so, although they follow direct decay paths to the origin, they do not appear to be remagnetized by lightning.

Low-stability components were fit for each sample, but they are scattered in a general southwestern direction and do not provide a mean direction with reliable Fisher statistics. Also, there is no consistency in directions amongst the two lithologies of anorthosite—we might expect the directions to be consistent within each rock type, but there is no pattern to the locations of the low-stability components in this site. This is true for the high-stability components, as well. Since decay to origin was apparent in the orthographic plots for these samples, most were fit with MTO lines. Only two, samples D and F, were fit to stable endpoints (SEP and HPL fits made). Irrespective of whether SEP or HPL fits are used in Fisher statistics calculations, a mean direction is not clear for this site, and there is no consistency within rock types.

INTERPRETATION: This site will not be used toward the calculation of a Kunene paleopole since the mean directions for both low- and high-temperature components are not well-clustered. Although the site is split between light and dark anorthosite, there are no noticeable patterns between directions derived in principal component analyses within each geological unit. This was probably not caused by lightning due to initially low magnetic moments in the samples, and remains enigmatic.

K04: The area in the previous three sites is sampled further away from dyke K01, in sites K04 and K05 situated on top of the river bank just above site K03. Site K04 contains nine samples of the dark anorthosite. All samples begin with moderate to weak magnetic moments (on the order of 1e-04 to 1e-06 emu) except for sample C, which begins at ~1e-02 emu. Low-stability components were fit for all samples, and cluster in a generally northwesterly mid-inclination downward direction (Figure 9). Sample C is an outlier with a southerly upward direction, and sample D has a northwesterly upward direction. With tilt correction, this cluster moves westward and all directions become northwesterly and shallow. Using all samples besides C and D gives reliable Fisher statistics, and further excluding samples E and F lowers the a95 value to ~16.

The high-stability components are clustered in this same direction. Most samples were fit with MTO lines, while two (C and F) were fit with DTO lines since the temperature at which demagnetization begins is outside the range of magnetite-like unblocking temperatures. The high-stability component for sample A was not fit at all due to scatter in data (error was too large to be useful). One sample, B, was fit with a SEP line and a HPL arc. Using seven of nine total samples gives a mean direction in a northwesterly mid-inclination downward direction (northwesterly shallow downward and upward when tilt corrected) with reliable Fisher statistics (Figure 8).

INTERPRETATION: The consistent low- and high-stability component directions across all samples would appear encouraging for paleomagneic stability, but the NW-down direction is similar to the direction found only in low-stability components by the K01 syenite dyke. As discussed in the next site description, this NW-down direction is interpreted as an Early Cambrian overprint affecting both the dyke and its anorthosite host..

K05: Located directly next to site K04, this site contains nine samples of the coarse, light anorthosite that is layered with the dark anorthosite. All samples start with moderate magnetic moments and are demagnetized through magnetite-like unblocking temperatures. Most low-stability components lie in a northwesterly moderate downward direction, which tilt corrects to northwesterly and shallow. The major outliers to this cluster are sample D, in a geographically

west-southwesterly upward direction, and sample C, in a geographically south-southwesterly downward direction. Without these, Fisher statistics are reliable for the low-temperature component mean direction.

The high-stability components were fit with MTO lines (except for sample C, which was fit with a DTO line). Samples C and D were again outliers to a main cluster in the northwesterly mid-inclination downward direction, which tilt corrects to northwesterly shallow downward and upward. This cluster also provides reliable Fisher statistics (Figure 8).

INTERPRETATION: Both the low- and high-temperature components of these nine samples cluster in the northwesterly shallow downward direction (geographic coordinates), similar to that observed in sites K01 and K04. Because the direction is observed in low-stability components at all three sites, it is interpreted here as a post-tilting overprint. The direction is similar to that expected from Early Cambrian time, according to the Gondwana apparent polar wander path (Mitchell et al., 2010). As the nearby Kaoko and Damara belts were orogenically active in late Ediacaran to early Cambrian time (e.g., Prave, 1996; Gray et al., 2006), hydrothermal activity in the Kunene region at that time is not unreasonable to postulate.

K06: This site contains nine samples of dark anorthosite in a locality with igneous layering. All nine samples begin with moderate magnetic moments (on the order of 1e-04 or 1e-05 emu) and are demagnetized to magnetite-like unblocking temperatures. All samples undergo a large drop in intensity at the liquid nitrogen step, which is indicative of the existence of multi-domain magnetite. Also, looking at orthographic projections for each of the sites, the main component of magnetism does not decay in a straight line to the origin, but rather a path that curves around to approach the origin. This could be evidence that the main component of magnetism (the high-stability component) is contaminated by a strong low component. This low component was fit for all nine samples, but no dominant cluster of directions for this component is apparent. In order to decide which samples are most reliable and thus provide mean component directions representative of the site, the magnetization after the LN2 step, relative to the NRM, was calculated. Lower ratios correspond to greater proportions of multi-domain magnetite among samples, and thus lower reliability of those data. According to this, samples C, E, F, and I have the highest LN2 to NRM moment ratios, which means they may be more reliable. Looking at the low-stability component directions, though, these four samples are split between west-northwesterly shallow downward and westerly steep downward directions, in geographic coordinates. With a tilt correction, these four form a loose cluster, mostly in a westerly shallow upward direction.

INTERPRETATION: High-stability components were fit for all samples except for one (F), which had an erratic decay to origin. All were fit with MTO lines except for two (A and H), which were fit to stable endpoints and high planes. The high-temperature components across all samples, using SEP fits or using HPL fits, are highly scattered but contain a loose cluster with steep upward direction in tilt-corrected coordinates (Figure 10). Despite the large error associated with this mean direction, its thermal stability, as evidenced by MTO linear fits through narrow unblocking temperature spectra indicative of near-stoichiometric single-domain magnetite, suggests that it can be used in calculation of a Kunene mean paleomagnetic pole.

K07: The first sample in this site, A, went missing during the sample preparation process, so the site consists of seven total samples. These samples were taken from a large pyroxene pegmatite—many of them broke apart along cleavage planes during preparation and had to be glued back together multiple times. All begin with magnetic moments on the order of 1e-04 emu and are demagnetized to magnetite-like unblocking temperatures. Most exhibit distinct low-stability and high-stability components, which are fit with LOW and MTO lines, respectively. Sample B is the only exception to this, as it produced messy data and required SEP and HPL fits for the high-temperature component. In both geographic and tilt-corrected views, the low-temperature components are scattered and provide no useful information about a mean direction. The high-temperature components show a loose clustering toward southeast and down, in tilt-corrected coordinates, although the Fisher statistics are large ($a95 > 20$).

INTERPRETATION: These pyroxene samples produced messy data, which led to only a loose consistency in mean directions for both low- and high-stability components of magnetization across the site (Figure 10). This could be due to the unusual lithology or to the fact that many of the samples were falling apart throughout the measurement process and needed to be re-measured due to errors many times. Despite the large error of the site-mean, a preponderance of steep downward high-stability components at this site allow it to be included in final Kunene pole calculations.

K08: Seven samples of dark anorthosite were taken from this site, all of which were demagnetized to magnetite-like unblocking temperatures. Sample G started with a weak magnetic moment (~1e-07 emu), but the rest of the samples had moderate initial intensities. A low-stability component was fit for each of the samples, but mean directions determined through principal component analysis are not consistent across the site. In both geographic and tilt corrected reference frames, the majority of these low-stability component directions lie in a northerly shallow direction, both upward and downward. However, these data points span a broad area on the equal

area stereonet projection, leading to poor Fisher statistics. The same is true for the high-stability components across the site. All samples except for G showed a direct decay to origin and were fit with MTO lines. These also span a broad area on the equal area stereonet projection and give poor Fisher statistics. Since no consistent direction is found, this site cannot be used any further.

INTERPRETATION: Seven samples of dark anorthosite were demagnetized to magnetite-like unblocking temperatures, but show no clustering of mean directions of either the low- or high-stability components. Therefore, the site should not be used in the calculation of a Kunene paleopole.

K09: A roadside streambed provided an outcrop of anorthosite with mafic layers and foliation in a northwest/southeast direction, from which nine samples were taken. Exposure of these mafic layers shows almost no elongation, which is evidence that the rock did not undergo sufficient metamorphism for remagnetization. All samples start with moderate magnetic moments around 1e-03 emu, and most (all except for I) are demagnetized to 610°C, just past the magnetite unblocking temperature. All have low-temperature components which, except for sample I, cluster mostly in a northeasterly steep downward direction. Applying a tilt correction moves this cluster northwestward so that the mean direction is north-northwesterly steep downward.

High-temperature components were fit with DTO lines (except for A, which was fit to a HTO line) and form a tight cluster in an east-southeasterly steep downward direction. With a tilt correction, this cluster is located in a northwesterly steep downward direction. Again, sample I is the major outlier to the cluster, with an upward direction in nearly the opposite polarity of the main cluster. Since these high-stability components produce reliable Fisher statistics using eight of nine samples (a95 = 10), this site could be used in further analysis.

INTERPRETATION: Both low- and high-stability components from eight of nine samples in this site have mean directions that lie in a statistically reliable cluster. The major outlier, I, has a high-stability component in the opposite polarity, has the lowest unblocking temperature, and is the only sample in the site that comes from a mafic enclave within the surrounding dark anorthosite. This is an intriguing aside, as it may be a record of a polarity change during cooling and tilting of the western Kunene region, or some other complicated sequence of intrusion and tilting left to be examined at a later time. The only difficulty with interpreting this site is the application of a tilt correction. As will be noted again in the discussion for site K11, the igneous layering of sites K09-K11 vary considerably over a lateral distance of merely a few hundred meters; this suggests that at

least one of the layering attitudes is likely unrepresentative of a paleohorizontal at the time of remanence acquisition.

K10: Located approximately 100 meters to the southwest of K09, this site also contains samples of dark anorthosite. All eight samples were run past magnetite unblocking temperatures and into hematite-like demagnetization temperatures. Sample C was run to 625°C, samples A and D were run to 666°C, and the rest were run to either 685°C or 695°C. Within this large range of temperatures, three separate components were determined for each sample, fit with LOW, MTO, and HTO lines. However, none of these components yield a statistically reliable mean direction, leading to poor Fisher statistics and rendering the site unsuitable for further analysis.

The low-stability components for all samples have geographic directions with moderate inclination that span from easterly to northerly, both upward and downward. With a tilt correction, these directions span from northwesterly to easterly at all inclinations, mostly downward. No mean direction can be determined from this set of low-temperature component directions. Both high-temperature components (MTO and HTO) are also scattered across a large area on the equal area stereonet projection. For all sites, the MTO component directions nearly overlap the HTO component directions. Geographically, these are mostly downward and lie at all inclinations in the eastern half of the equal area stereonet. With a tilt correction, the directions span the southern half of the stereonet from east to west at all inclinations. This poor clustering leads to unreliable Fisher statistics, so none of the components of magnetism from this site should be used further.

INTERPRETATION: These eight samples of dark anorthosite produce dissimilar directions to the dark anorthosite samples from site K09, which is unexpected since the sites are in such close proximity. However, the clustering in this site is poor, so any mean direction calculated here will be more unreliable than the mean directions from the low- and high-stability components of site K09. Therefore, this site will not be used in further calculations of a paleopole.

K11: This site lies 50 meters to the southwest of K10 and also contains eight samples of dark anorthosite. Sample D was run to 595°C, sample E was run to 610°C, and sample H was run to 666°C, while the rest of the samples had a substantial hematite component and were run to either 685°C or 695°C. All samples begin with moderate magnetic moments on the order of 1e-02 or 1e-03 emu, and all contain a low-temperature component that was fit with a LOW line. These low-temperature components lie mostly (five of eight samples) in a westerly steep downward direction, in geographic coordinates. With a tilt correction, this cluster moves to a west-southwesterly shallow downward direction. Three different labels were used to classify the decay to origin fits for

the high-stability components in these samples. Sample D was fit with an MTO line, samples B, C, and E were fit with DTO lines, and samples A, F, G, and H were fit with HTO lines, the difference in classification here being the starting temperature of decay toward the origin. Again, after excluding three points (A, E, and F—the same samples excluded from the low-temperature cluster), a cluster of directions mostly westerly steep downward can be determined. With a tilt correction, this cluster moves into a west-southwesterly shallow downward direction. Although this site provides a much clearer mean direction for dark anorthosite than site K10, it does not agree with the direction found in K09 and Fisher statistics are not considered reliable (a95 = ~24).

INTERPRETATION: The majority of the samples in this site contained a substantial hematite component, so HTO and DTO line fits were used in determining the mean directions for most of the high-stability components across the site. Although directions did cluster to a degree, the Fisher statistics of this cluster are not reliable, and the mean direction does not match the direction given by the dark anorthosite in site K09 (Figure 11). The discrepancy in igneous layering attitudes between sites K09 and K11 is puzzling, given their close proximity. The two high-component site means are closer to each other in geographic coordinates than upon rotation of the igneous layering to horizontal. If the layering is not to be used as a paleohorizontal datum, then all sense of tilt control is lost at this locality. Therefore, the data from sites K09-K11 are not used in calculation of a mean Kunene paleopole.

K12F: This site contains ten samples from the felsic cobbles of a conglomerate outcrop that stretches approximately 15 meters in length. Bedding is subhorizontal in fine-grained siliciclastic sediments decameters above the conglomerate unit. Samples were demagnetized to temperatures between 590°C and 665°C, and directions determined through principal component analysis for both low- and high-temperature components were inconsistent across the site (as expected for a conglomerate). Low-stability components are mostly upward and steep, but lie at all declinations (both geographically and tilt-corrected). High-stability components were fit with DTO, MTO, or HTO lines depending on the temperature at which demagnetization toward the origin begins. The directions of these components are also mostly upward, but span a large range of inclinations and declinations. All samples had an initially moderate magnetic moment on the order of 1e-04 emu (Figure 12).

INTERPRETATION: This site includes ten felsic samples from a conglomerate that are to be used in combination with the samples from K12M in a conglomerate test. The mean directions determined here will not go into the calculation of a Kunene pole. The fact that there is no main

cluster of low- or high-stability component directions supports the hypothesis that each individual cobble maintained a ChRM direction from times prior to becoming part of the conglomerate, and that the entire unit was never remagnetized as a whole. Two clasts were doubly sampled by two adjacent, independently oriented cores. Within each clast-pair, data are generally reproducible, enhancing the reliability of the positive conglomerate test.

K12M: This site contains 15 samples from the mafic cobbles of the same conglomerate site as K12F. Similar results as the previous site are found in this set of samples, in that both low- and high-stability component directions are scattered and do not suggest a coherent mean direction. All samples began with relatively weak magnetic moments (most on the order of 1e-07 emu) and were demagnetized to magnetite-like unblocking temperatures. The low-stability components are completely scattered (both geographically and with applied tilt correction) across declinations and inclinations. High-stability components, which were fit with either DTO or MTO lines, also have directions that are spread across the equal area stereonet. The spread of directions, though, looks different than the random spread seen in K12F, suggesting that this conglomerate unit also passes the conglomerate test (Figure 12). Same-clast pairs don't show as consistent results as the pairs from K12F, but overall, between-clast scatter remains much larger than within-clast scatter.

INTERPRETATION: Combining results of this site and the previous (which are of one large site split into two based on composition) demonstrates a positive conglomerate test. This is useful in knowing that rocks from this area have not been remagnetized, but the strength of the test depends on the age of the conglomerate, which will be discussed below in the section on field stability tests.

K13: Eight samples of dark anorthosite were taken from a variably altered and veined unit with layering defined by a persistent south-dipping pegmatite horizon. All samples begin with moderate magnetic moments on the order of 1e-03 emu, all are demagnetized to 590°C, and all have a low-temperature component fit with a LOW line and a high-temperature component fit with a MTO line. The low-temperature components show a consistent cluster of directions across the entire site, with most of the directions falling in a southwesterly upward direction, geographically. With a tilt correction, this cluster moves northward to a northwesterly upward direction. The high-temperature components also show this northward movement after tilt correction. This cluster of directions lies geographically in a south-southwesterly very steep upward direction and moves to a north-northwesterly mid-inclination upward direction. These clusters are well defined and provide reliable Fisher statistics ($a95 < 20$), so this site should be used in further analyses.

INTERPRETATION: The mean directions for this dark anorthosite (north-northwesterly mid-inclination upward) are well clustered and derive from data with narrow unblocking-temperature spectra indicative of single-domain magnetite. Site K13 will therefore be used in the final analysis of the Kunene Complex (Figure 13).

K14: Located along the southern border of the Zebra Mountains, this site contains another eight samples of dark anorthosite which all begin with magnetic moments on the order of 1e-02 or 1e-03 emu and are demagnetized to magnetite-like unblocking temperatures. Much like K13, all samples in K14 have a low-temperature component fit with a LOW line and a high-temperature component fit with either a MTO or DTO line (half of samples were demagnetized to 585°C, while the other half was run to 610°C). Low-temperature component directions for each sample fall into a well-defined cluster that is located geographically in an east-northeasterly steep downward direction. Applying a tilt-correction shifts these directions southward so that the cluster lies in a southeastern mid-inclination downward direction. Reliable Fisher statistics are calculated for this cluster using all samples.

The high-stability component directions seem to lie in nearly the exact same positions as the low-stability component directions, suggesting that this low-stability component may not be entirely separate. Geographically, the high-stability component directions all lie in an easterly steep downward direction, which shifts southward to a south-southeasterly mid-inclination downward direction after applying a tilt correction. Fisher statistics for this cluster of directions suggest that this site is reliable, so it will be used in further analysis of a Kunene paleopole (Figure 13).

INTERPRETATION: Site K14 yielded the most consistent and narrow unblocking-temperature directions from any Kunene site. Its direction is of roughly opposite polarity to that of K13, which is located laterally a few km to the west. Both sites are used in Kunene pole calculation, and the overall excellent magnetic behavior from this area at the southern flank of the Zebra Mountains would be most prospective for further sampling and pole refinement.

K15: The eight samples taken from this site are divided into two groups based on outcrop location and composition. Samples A through D were located at the bottom of a ridge, are dark in color, and contain randomly oriented plagioclase crystals. Samples E through H were located about 20 meters away from the first four samples, are also dark in color, and contain plagioclase crystals that are all oriented in the same direction. During the preparation stage of this site, sample E was never found, so it was either lost in the field or in transportation to the lab. The other seven samples all begin with relatively strong magnetic moments on the order of 1e-02 emu and contain both low-

and high-stability components. Samples A through D were demagnetized to either 585°C or 590°C, while F through H were demagnetized to 665°C.

The low-temperature components from this site all lie geographically in a northeasterly shallow direction, both upward and downward. With a tilt-correction, this declination remains the same, but samples A through D are downward while samples F through H are upward. This pattern is maintained in the tilt-corrected directions of the high-stability components. However, the clustering of these directions is not well defined and not statistically reliable, so it won't be used for further calculations. With a tilt-correction, four of the seven samples have directions that lie in a northerly shallow direction.

INTERPRETATION: There are obvious differences in low- and high-stability component directions between the first half of this site (randomly oriented plagioclase crystals) and the second half (oriented crystals). Samples A through D have component directions that do not cluster at all—they lie at all declinations around an equal-area stereonet. The rest of the samples' component directions cluster generally in a northerly shallow direction. Although this site will not be used toward a Kunene pole, it may be important in describing the dominant geological processes in this area, especially those that may have affected crystal orientation throughout the unit.

K16: Eight more samples of dark anorthosite were collected at this site, not far from a river crossing by the main track at the southern edge of the Zebra Mountains; all of the samples have aligned plagioclase crystals like the second half of samples from K15. All begin with moderate magnetic moments on the order of 1e-03 emu and are demagnetized to either 585°C or 595°C. Every sample has a low-temperature component fit with a LOW line as well as a high-temperature component fit with an MTO line. Most low components start geographically in a northerly shallow downward direction, and then tilt correct to become steeper with the same declination. This cluster is not tightly defined, as samples B, C, and G are outliers that lie to the south of the main cluster of directions. The high-stability components, on the other hand, are all tightly clustered and provide a statistically reliable mean direction. Geographically, the directions of this component in all samples are generally southerly mid-inclination and downward. With a tilt-correction, these directions become shallower and the majority lies in a southerly shallow upward direction. This produces reliable Fisher statistics (a95 ~15), so the mean direction of the high-stability components may be useful for further Kunene paleomagnetic pole characterization (Figure 13).

INTERPRETATION: Comparing the mean direction of these samples with the compositionally similar samples from K15 (F through H) suggests that the two could be of opposite

polarity. However, this north-south direction is unlike the other dark anorthosite directions seen in previous sites. Since this site shows good clustering with reliable Fisher statistics, it could be used for further Kunene characterization, even though it is not similar to previous sites. However, it is outlying relative to the other robust sites, so it may represent a geomagnetic excursion.

K17: More veined dark anorthosite from along the southern edge of the Zebra Mountains is sampled at this site. Seven samples were taken from areas of the outcrop that did not seem to be magnetized (surrounding areas were magnetized). All samples start with moderate magnetic moments between ~1e-02 and ~1e-03 emu, and most are completely demagnetized by 590°C. Sample B is the exception to this, as it was run to 640°C and also has the largest initial magnetic moment. All samples have a low-temperature component, which is fit with a LOW line, as well as a high-temperature component fit with a MTO line. Geographically, the low-temperature component directions are all in the northeastern quadrant of the least squares equal area stereonet, but span a range of inclinations. All are upward except for samples A and G, which are steep downward. With a tilt correction, A and G move southward to a moderate inclination while the other samples all move to a northeast shallow downward direction (except B, which remains upward).

The high-temperature component directions are also mostly upward with two outliers (samples A and C) in a geographic projection. Most samples have directions in an east-southeasterly shallow direction, and, with a tilt-correction, they shift northward to become eastward and shallow upward. Fisher statistics for this cluster are not reliable, so this site will not be used to characterize the Kunene paleopole.

INTERPRETATION: The mean directions given in this site are not well defined, making them statistically unreliable and unsuitable for further analysis. The mean directions for this site resemble more closely the high-stability component directions from the Swartbooisdrif region, which means, if K17 is reliable, it may actually be part of a younger intrusion and not part of the Kunene unit.

K18: Eight samples from what appeared to be a dark mafic sill were taken from this site, although the bounding attitudes of the intrusion were not well exposed. All of the samples start with a relatively strong magnetic moment on the order of 1e-01 or 1e-02 emu. All samples were demagnetized to temperatures 600°C or higher, and all had separate low- and high-temperature components fit with LOW and DTO lines, respectively. Most low-temperature component directions span the entire range of declinations in the southwestern quadrant of the equal area

stereonet. Most are shallow and upward with the exceptions of sample D being shallow and downward and sample B being in a northeasterly direction. Because of this range of declinations, the geographic cluster of directions is not well defined. With a tilt correction, the majority of directions moves northward and spans a smaller range of declinations in a west-southwesterly shallow direction.

The high-temperature components follow a similar pattern, with all directions spanning a range of declinations in the southwestern quadrant of the least squares equal area stereonet. With a tilt correction, these directions move northward, and the densest cluster of directions is in a west-southwesterly shallow upward direction. Only three samples (C, D, and F) are in a downward direction, and they all lie to the north of this cluster (west-northwesterly). The Fisher statistics for both low- and high-stability components are just outside the range of being reliable (a95 = 25 and 22, respectively), so this site may be considered for further analysis.

INTERPRETATION: The high-temperature component directions for six of eight samples in this site cluster in a generally west-southwesterly shallow upward direction. Although the cluster is not very well-defined, Fisher statistics are good enough that this mean direction could be used in further characterization of a Kunene pole if more data were to be gathered. However, the direction is also similar to those from Swartbooisdrif dykes (see below), suggesting the possibility that the K18 intrusion could also be an intrusion substantially younger than the Kunene Complex itself.

S04. This site is from unbaked Kunene complex anorthosite in the Swartbooisdrif region, and its mean remanence direction will be used in calculation of a Kunene paleomagnetic pole. However, it constitutes part of a baked-contact test with a younger Swartbooisdrif dyke, so the magnetic behavior will be discussed below, in the section on Swartbooisdrif dykes.

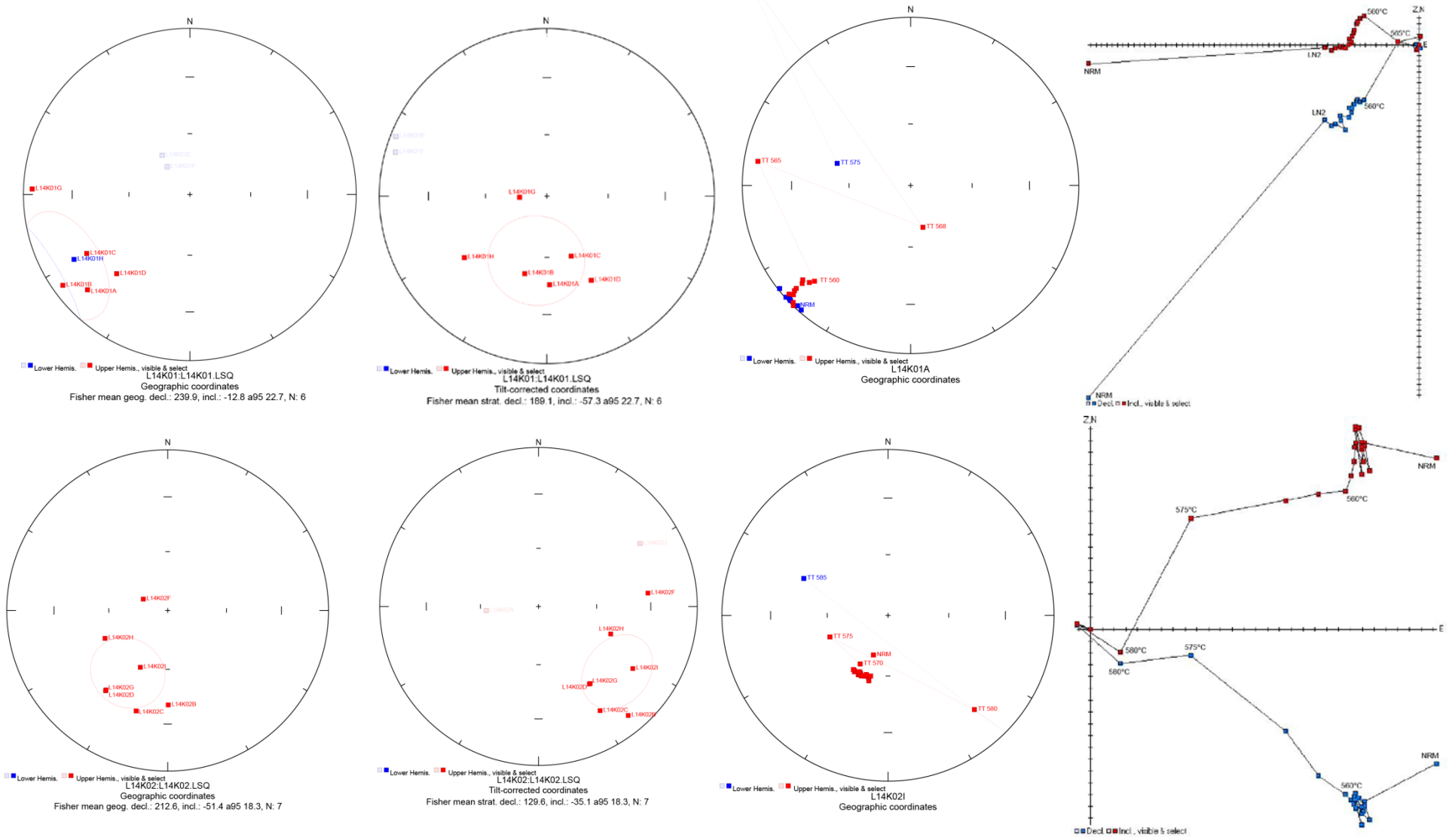

Figure 7: These two sites are a dyke (L14K01, top) and its immediate anorthosite host rock (L14K02, bottom). Each row, from left to right, shows the mean high-stability direction (*in situ* and tilt-corrected for the host anorthosite layering) with Fisher statistics 95% confidence ellipses, equal-area stereonet plot for a representative sample, and an orthographic Zijderveld plot for that sample.

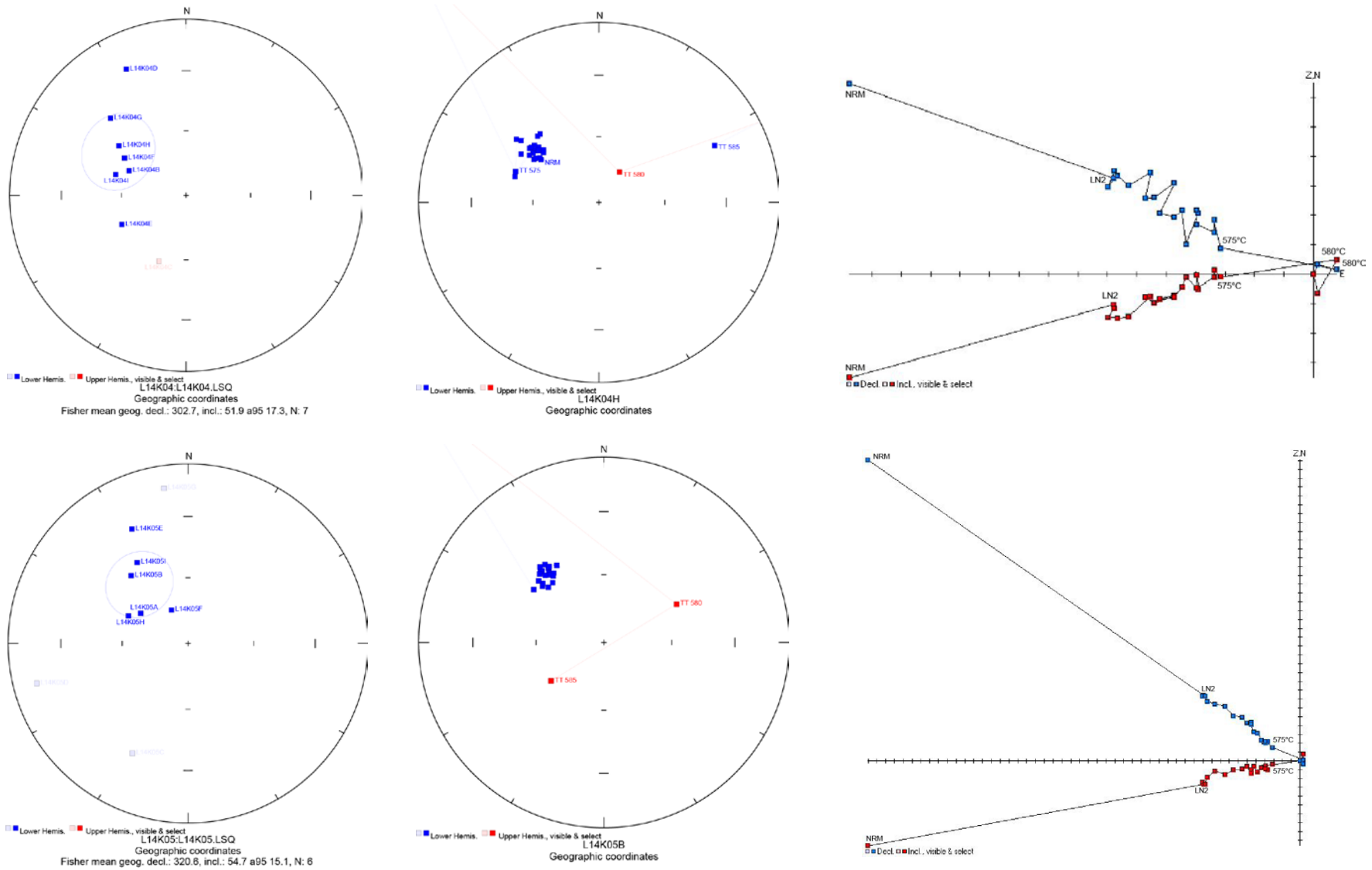

Figure 8: The top row, from left to right, shows the mean high-stability direction with Fisher statistics 95% confidence ellipse, equal-area stereonet plot for a representative sample, and an orthographic Zijderveld plot for that sample, all from site L14K04. The bottom row contains the same three plots for site L14K05. Note the similarity between these two geographic mean directions and the low thermal directions in Figure 9, suggesting that this northwest-down direction is an overprint.

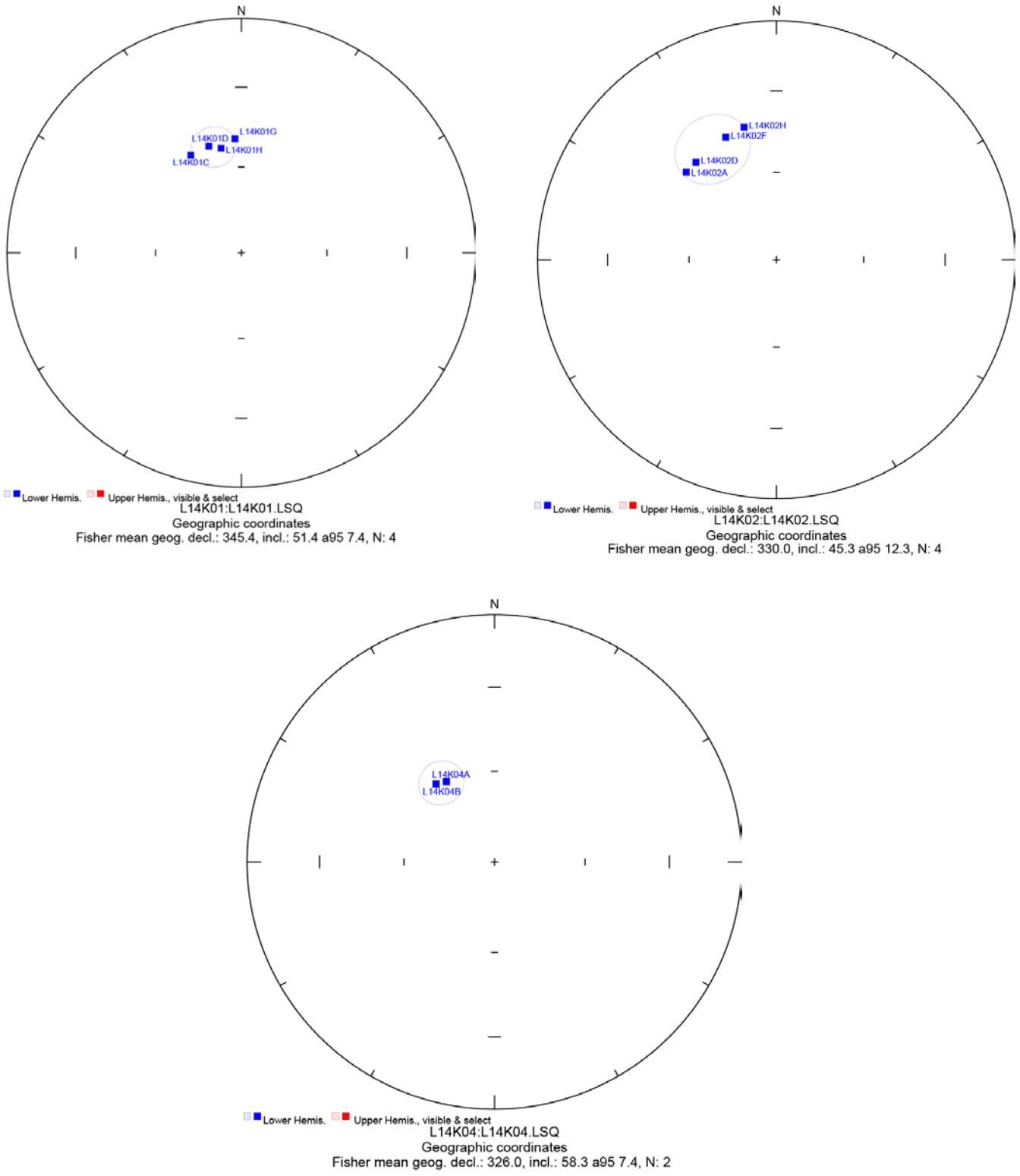

Figure 9: Sites L14K01, L14K02, and L14K04 all contain a low thermal component which lies in the same geographic direction, as seen in the three stereonets here. This mean direction is similar to the mean direction in sites K04 and K05 (Figure 8), suggesting that this is an overprinted direction that is younger than the dyke from site K01. Therefore, none of these sites were used in the calculation of a Kunene paleomagnetic pole.

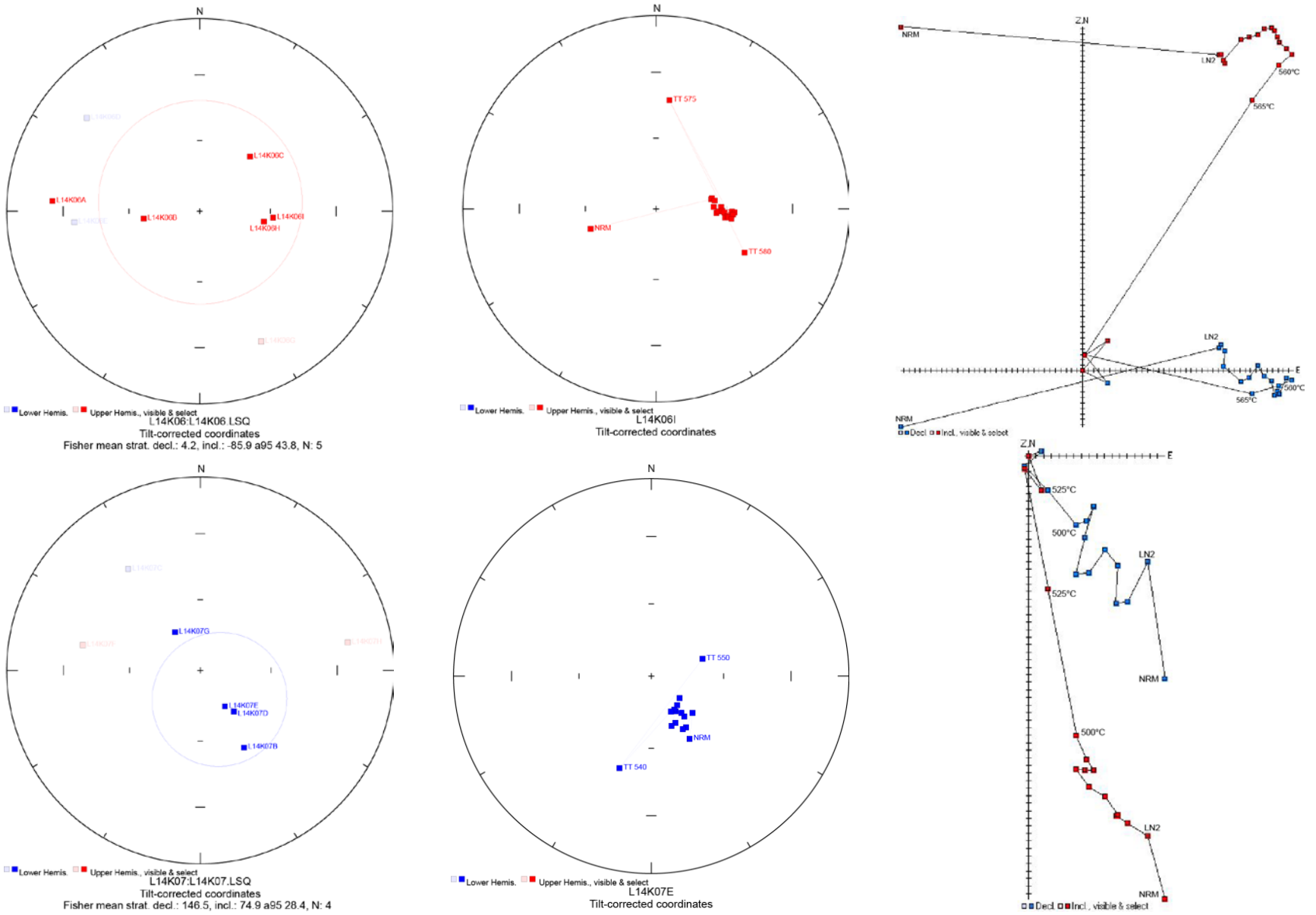

Figure 10: Sites L14K06 and L14K07 are both used in the calculation of a preliminary Kunene pole. The top row, from left to right, shows the mean high-stability direction with Fisher statistics 95% confidence ellipse, equal-area stereonet plot for a representative sample, and an orthographic Zijderveld plot for that sample, all from site L14K06. The bottom row contains the same three plots for L14K07.

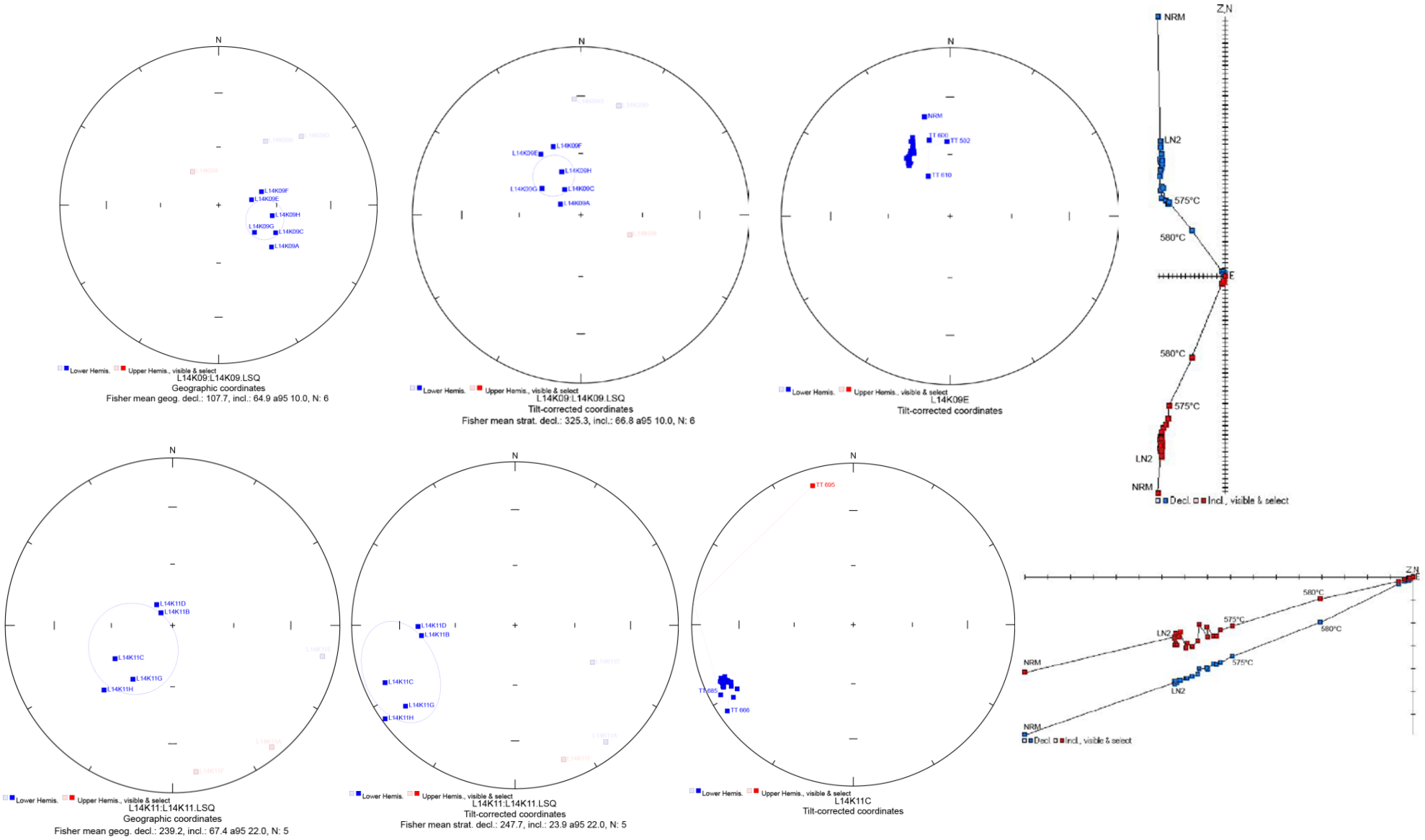

Figure 11: These two sites (L14K09 top row, L14K11 bottom row) were not used in the calculation of a Kunene paleopole, but demonstrate the problems with tilt correction within the site—directions diverge instead of converging. From left to right are geographic and tilt-corrected mean high-stability directions, equal area stereonets for representative samples, and orthographic Zijderveld plots for those samples.

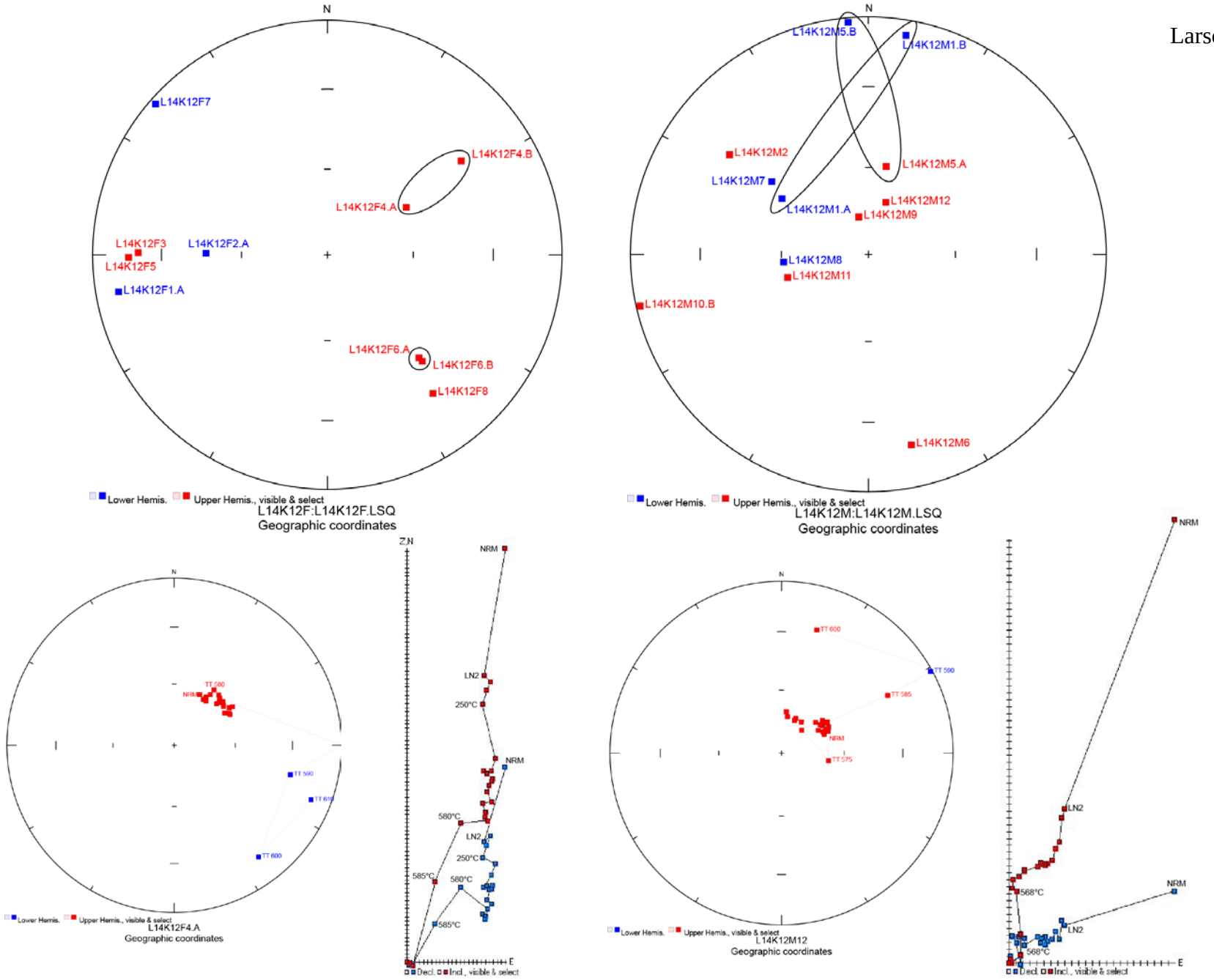

Figure 12: L14K12F and L14K12M were collected from the same location to be used in a conglomerate test. The high-stability components of all samples in each site (top row) show no consistency in direction except for those taken from the same clast in L14K12F, proving a positive conglomerate test. Because samples from the same clast produced different mean directions, L14K12M is not used in the conglomerate test. The bottom row shows an equal area stereonet and an orthographic Zijderveld plot for a representative sample from each site.

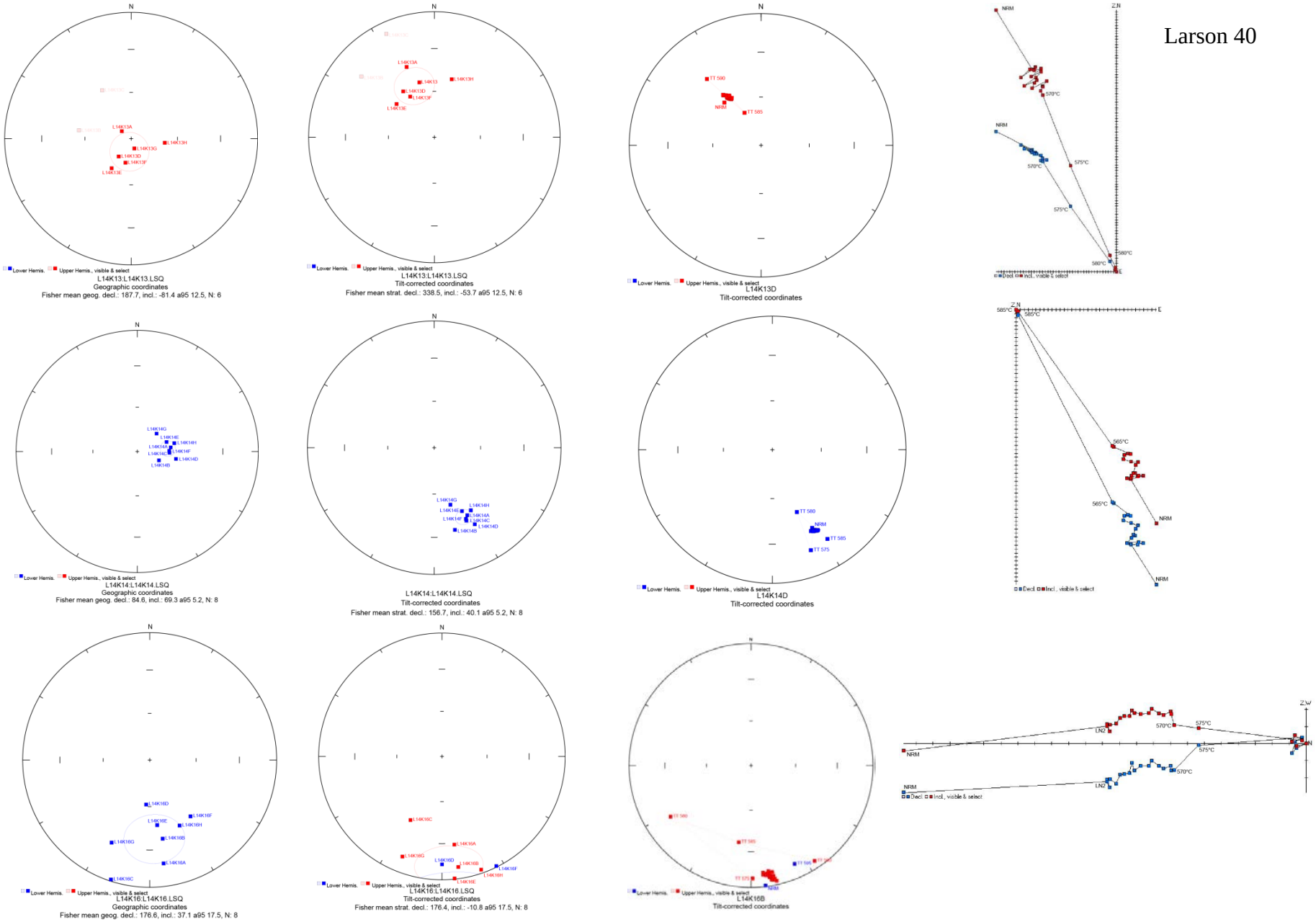

Figure 13: Two more sites used in the calculation of a preliminary Kunene pole are shown here, as well as a stable but outlying site mean (L14K16). The top row, from left to right, shows the mean high-stability direction with Fisher statistics 95% confidence ellipse, equal area stereonet plot for a representative sample, and an orthographic Zijderveld plot for that sample, all from site L14K13. The second row contains the same three plots for site L14K14 (the tightest-clustered site of all Kunene sites), while the bottom row contains plots from directionally

Swartbooisdrif Dykes

Thirteen sites were sampled from the Swartbooisdrif area, five of which provide data contributing to a mean high-stability direction for the unit. Data plots for these sites are shown in figures 14 and 15.

S01: Nine samples were taken from a riverbed outcrop of a pink, feldspathic carbonatite dyke. All samples except for one (C) show substantial demagnetization between 560 and 570°C, and most have NRMs with a moderate magnetic moment (~1e-05 emu). However, most samples do not decay to the origin and were fitted to stable endpoints (SEP) and high planes (HPL). Although intensity plots suggest magnetite-like unblocking temperatures for the majority of the samples, clear decay toward the origin is hardly seen in this site, as all high-stability components are messy and appear very scattered on orthographic Zijderveld diagrams. Only one decay-to-origin (DTO) fit is made (sample G), and it spans steps 300°C through 520°C since all higher temperature steps are unusable. Sample C is completely demagnetized by 625°C, suggesting the presence of hematite. The higher temperature steps for this sample are also scattered and unreliable, so they were fit with a SEP and a HPL. Nonetheless, the low-stability components are relatively consistent between samples, with six of seven sites plotting in a north-northwest, moderately shallow, upward direction.

INTERPRETATION: While the low-temperature components are consistent between samples, high-temperature components are unusable for this site. The higher-temperature steps produced messy data, so only one decay-to-origin fit could be made. The other stable endpoints and high planes do not provide any conclusive direction for the final demagnetization components.

S02: This site is located only 15 meters away from S01 in the same riverbed, and contains seven samples of a fine-grained, gray carbonatite dyke (which intrudes the anorthosite sampled in S03). Samples A, B, D, E, and F start with a strong magnetic moment around 1e-01 emu, while C and G have more moderate moments around 1e-04 emu. This majority of samples that are strongly magnetized at the NRM step require heating to 610°C (654°C for B) for complete demagnetization, while C and G were only heated to 590°C. All samples are single-component and demagnetize directly to the origin, so DTO fits were made for all seven. There are no low components that are distinguishable from the main magnetic component, so no LOW or LTH fits were made for the site. Looking at intensity plots shows that, although the NRM steps have high initial magnetic moment, lightning is not an issue in this site—all show decay quickening around magnetite-like unblocking temperature. Five of seven high-stability components have a consistent easterly shallow upward direction, forming a tight cluster with reliable Fisher statistics. Samples F and G give components

in the same azimuthal direction, but are downward, so these are excluded from Fisher statistics (Figure 14).

INTERPRETATION: Five of seven samples show a consistent easterly shallow upward direction for the high-stability component of demagnetization, and the Fisher statistics of this cluster will contribute to a VGP and, with more data, a preliminary Swartbooisdrif paleopole. Although the samples started with high magnetic moments, intensity plots show no evidence of lightning interference at the site. No low components were fit since they were not distinguishable from the rest of the demagnetization process. If site S03 shares the same high-stability component direction, this will be part of a positive baked contact test.

S03: Carbonatite from S02 intrudes mottled green-gray anorthosite, from which seven samples are taken for site S03. Since this anorthosite is in immediate contact with the carbonatite, we should expect the high-stability components of these samples to have the same direction S02, which would contribute to a paleomagnetic baked-contact test. All samples besides A (which was noted to contain small amounts of carbonatite) start with strong magnetic moments around 1e-01 emu (in contrast to an initial moment for A of ~1e-05 emu), and most samples retained magnetization to 695°C as a hematite component. Only two low-stability components are distinguishable (sites A and G), so Fisher statistics were only calculated for high-stability components. All sites were fit with DTO lines, and an easterly shallow upward direction is observed for four of the seven sites. The other three sites (E, F, G) have the same easterly shallow direction, but are opposite polarity (downward).

INTERPRETATION: S03 is part of the same anorthosite unit as S02 (but is far removed from younger dykes) and also has a majority of samples which begin with high magnetic moments. The high-stability (hematite) components in four of seven S03 samples have the same easterly shallow upward direction as the majority of S02 samples, which may be proof of a baked contact test. However, there are three outliers that share the same azimuthal direction, but are downward instead of upward. By comparing the loss of magnetic moment that occurred at the LN2 step for all samples, the multi-domain ratio is calculated and shows which of these two groups is more likely to be representative of the site. In this case, the four upper hemisphere components have a lower mean ratio and are less likely to be dominated by multi-domain magnetite, making them more suitable for paleomagnetic study. Therefore, Fisher statistics for this cluster (Figure 14) will be used in determination of a paleopole. Also, this site, in combination with S02, contributes to a positive baked-contact test. Both units share the same high-stability component direction, which is evidence

that the host rock (S03) magnetization was completely reset upon emplacement of the adjacent younger dyke (S02).

S04: Six samples of unaltered anorthosite were collected about 50 meters away from sites S01-S03. Although the anorthosite is unaltered, it is noted that a south-dipping carbonatite sill is located about five meters to the south and projects northward two to three meters above the site. All six samples are completely demagnetized at a magnetite-like unblocking temperature (585°C), and begin with moderate magnetic moments (~1e-02 to ~1e-03 emu). Five low-temperature components were fit with lines, but there is no consistent direction amongst the sites, so these will not be used in further calculations. Two sites (A and B) were fit with mid-thermal components, which are northwest, steep, and downward. Looking at J/J0 plots, these mid-thermal steps may not be entirely separate components because the drop in magnetic intensity is not substantial and the unblocking temperature is around 500°C. However, this could also suggest that DTO components may be split between stoichiometric magnetite and some hematite, in which case separating components may be useful. By comparing the amount of intensity lost between the NRM and LN2 steps for all samples in the site, we were able to make an objective hypothesis about whether some samples have a greater proportion of multi-domain magnetite. A larger multi-domain contribution means the final direction of the high-stability component for that sample may not be reliable. In some cases, the mid-thermal component could be combined with the MTO fit from each site to create a DTO fit instead, but this did not significantly change the final direction.

Assuming these mid-thermal fits are accurate, four DTO and two MTO fits were made, which gives a bimodal distribution and unusable Fisher statistics. Both MTO fits (A and B) have a steep downward component, but A is north-northwesterly while B is west-northwesterly, leaving a large azimuthal discrepancy between the two. There is one DTO fit (C) for which the high-stability component lies directly between A and B with a steep downward direction. The other three (D, E, F) form a tighter cluster and are also steep and downward, but have an east-northeasterly direction. A spreadsheet to calculate the multi-domain ratios of these six samples was used to determine which three should be considered the accurate representation of this site. The spreadsheet takes in the magnetic moment values at the NRM and LN2 steps and uses the equation 1-(LN2/NRM) to find the ratio, where a ratio closer to 1 means a sample is dominated by multi-domain magnetite. With this method, the first three samples (A, B, C) have a lower mean ratio than the other four samples, so this cluster will provide the representative high-temperature direction for the site.

INTERPRETATION: It is important to note that this site is part of the Kunene unit. Most of the samples seem to have single DTO components, but, looking at intensity plots, may actually consist of magnetic contributions from both stoichiometric magnetite and hematite. Using single DTO components was determined most useful in this site, especially considering primary igneous magnetite may provide thermoremanent magnetization while hematite could be an effect of immediate post-cooling deuteric oxidation. Using these fits, neither the low-stability or high-stability components for this site show consistency across samples, but analyzing whether or not some samples may contain multi-domain magnetite helped objectively determine which samples are representative of site direction. The Fisher statistics from this cluster will be used in determining a Kunene paleopole. The complicated mid-thermal signature in two of the samples may be an indication of contamination, and this may be something to look into in the future. Lastly, this site completes the Swartbooisdrif baked contact test (Figure 14).

S05: Nine samples were collected from a weathered, mafic-rich carbonatite dyke surrounded by white anorthosite. Chilled margins between the two units are noted, and samples A-E are fine-grained rock while F-I are coarser-grained. All samples have a hematite-like unblocking temperature, with most samples being demagnetized until 695°C. The samples begin with magnetic moments on the order of 1e-02 emu and appear to be strong, single-component, hematite-bearing rocks. J/J0 plots show a hidden magnetite-like unblocking temperature, where a small drop in magnetization occurs around 550°C for each sample. However, only a single high component was fit for each sample (all DTO, which could possibly be split into MTO and HTO based on J/J0 plots—these would have the same directionality, though). Low-stability components were fit with lines for six samples (A, B, C, D, E, H) and do not show strong consistency between samples. While four of the six share a north-northeasterly upward direction, they range from shallow to steep, and the other two components are west-northwesterly and southeasterly. Fisher statistics were not calculated for this unusable set of low-stability directions.

The high-stability components are significantly more coherent, and Fisher statistics are calculated using eight of the nine samples. These eight are in a north-northeasterly upward direction, but range from shallow to steep. The ninth sample (A) is in the opposite polarity (south-southwestern, shallow, and downward). Fisher statistics are also calculated including the ninth sample, but reversing the polarity, which gives a comparable a95 value (14.8 vs. 17.2 with the ninth sample).

INTERPRETATION: While there was no consistency amongst the low-stability components of demagnetization across the site, the high-stability components are uniform and reliable Fisher statistics can be calculated. However, this site is not used in the calculation of a preliminary Swartbooisdrif paleopole.

S06: This site consists of nine samples taken from a weathered mafic dyke, all of which have magnetite-like unblocking temperatures around 585°C. All samples have moderate NRM moments (~1e-02 or 1e-03 emu), and seven of nine were fit with DTO lines (seem to be single-component). The other two sites (D and F) were fit with MTO lines since decay to the origin begins and ends in the range of magnetite unblocking—decay begins between 500 and 550°C and reaches full demagnetization around 580°C. In addition, eight of the samples were fit for low-stability components, but the directions of these are not very consistent across samples. Seven are in the upper hemisphere while one (B) is in the lower. The upward directed components are spread across the north and northwestern portion of the stereonet, and also span a range from shallow to steep. Sample B is in a southwestern steep direction. Fisher statistics are calculated without sample B, even though the error is relatively large.

The high-stability components are even less consistent, with three samples (B, D, I) in the lower hemisphere and the other six in the upper hemisphere. Most components again lie in either a north or northwestern direction over a range of inclinations, with the one outlier being sample B in a southeasterly steep direction. Fisher statistics may or may not be used here (auto-reverse lines?) since error is relatively large.

INTERPRETATION: Nine samples, all demagnetized at a magnetite unblocking temperature, provide somewhat consistent directions for both low- and high-stability components. This site may be used in the calculation of a preliminary Swartbooisdrif pole, but it will depend on how many other sites produce consistent directions since there is relatively large error in the Fisher statistics for this site. In the end, we decided not to include this site in our preliminary paleopole calculation due to the large error.

S07: Another weathered mafic dyke was sampled, and this time the nine samples collected were mostly demagnetized at a hematite-like unblocking temperature. Most samples in this group contain three separate components, so low or low-thermal (LOW or LTH), mid-thermal (MTH), and hematite-to-origin (HTO) fits were made for each sample. Intensity plots of J/J0 clearly reveal the boundaries between these components: the low-stability component starts with the NRM or LN2 step and ends around 300°C, the mid-thermal component spans some combination of temperature

steps between 400 and 580°C (magnetite-like unblocking temperature), and the high-stability component is above 580°C, indicating a hematite decay to origin. Each of these steps has some consistency throughout the site, indicating the patterns in which demagnetization took place.

All samples are similar in that they begin with magnetic moments on the order of ~1e-03 emu, and low components mostly (six of nine samples) in a northeasterly upward direction. Mid-thermal components were fit to six samples (A, B, C, D, F, G) and show a general westward migration from the low-stability components. Four of six mid-thermal components are in a northwesterly, steep upward position. HTO (or DTO, depending on where decay to origin began) fits were made for eight of the samples. Sample E provided mostly unusable data—it was only run to 565°C and the Zijderveld plot was very scattered. These fits cluster well in a northeasterly, shallow upward direction, with only one outlier. Sample F has a high-stability component which is in a southern, shallow downward direction, so this data point is not included in Fisher statistics for the site.

INTERPRETATION: S07 consists of nine mafic samples which clearly demonstrate multiple components of demagnetization. The high-stability components provide good Fisher statistics, either using eight of nine samples or using all nine, but reversing polarity of one. Fisher statistics on the low-stability components contain more error, but, using seven of nine samples (again reversing polarity of one), another virtual geomagnetic pole can be created. This site was not used in the calculation of a preliminary paleopole.

S08: Twelve samples of coarse dolerite with a wide range of initial magnetic moments (~1e-01 to ~1e-04 emu) were collected at this site, and, overall, provide scattered, inconclusive data. All were demagnetized to magnetite-like unblocking temperatures, and one sample (A) contained a hematite component and was demagnetized to 695°C. Low components were fit for eleven of twelve samples, but there is no consistent azimuthal direction across the site and a perfect split between upward and downward directions (five lower hemisphere, six upper). These cannot be used for any further analysis. The high-stability components are marginally more consistent, but still scattered. However, because there are twelve total samples, five or six data points can be eliminated so that the Fisher statistics will provide a mean direction which matches the mode of samples. Six DTO and six MTO fits were made, but no patterns emerge in the directionality of these components as a whole group or separate groups.

INTERPRETATION: The twelve samples in this site all provide many different directions for low-stability and high-stability demagnetization directions, however they are not completely

unsuitable for calculating a mean pole for the site. There is a small grouping of high-stability components toward the southwestern shallow direction, but a split between upper and lower hemispheres leads to large error in Fisher statistics. Disregarding half (six of twelve) of the samples leads to a well-defined cluster of mean high-stability directions which is included in a final pole calculation.

S09: There are eight samples collected from a dark mafic dyke in this site, and all are demagnetized past magnetite unblocking temperatures. Samples D and E start with strong magnetic moments on the order of 1e-01 emu, while the rest are on the order of 1e-02 emu. Samples A, B, C, and H have the lowest intensities overall. Low-stability components were fit for seven of the eight samples—the eighth (D) was single-component, where a low-temperature component could not be distinguished from the DTO path. The directions of these are not consistent across the site: samples A, B, and C give directions that are southern and shallow upward, but E, F, G, and H are all downward and range from northern and shallow to southeastern and steep. Because of this, the low-temperature directions are unusable for further analysis. However, there is a correlation between component directions and magnetic moments—the strongest samples (D and E) are located in a north-northeasterly shallow downward direction and the least strong (A, B, C, and H) are located in a southerly shallow upward direction (H is downward), leaving the remaining samples (F and G) directly between the two clusters. These groupings also mirror the locations from which samples were taken on the outcrop, and the samples show a large drop in magnetization at the liquid nitrogen step, which is indicative of multi-domain magnetite. It is likely, then, that lightning caused a localized remagnetization of these samples.

All of the high components were fit with DTO lines, but the discrepancy in directions amongst the samples remains. Again, A, B, and C are in a southern and shallow upward direction, while remaining samples are all downward following the same range of directions as previously mentioned. Fisher statistics with auto-reverse on samples A-E provide the lowest-error cluster of high-stability directions. Also, using the multi-domain equation spreadsheet, the most reliable cluster, and thus the cluster used for Fisher statistics, is the one including A, B, and C.

INTERPRETATION: Both the low- and high-temperature components show a wide spread in directions, and may or may not be useful in the calculation of a Swartbooisdrif pole. Using auto-reverse Fisher statistics for the high-stability components on five of eight samples produces a VGP with an a95 value of 13.9. This site is not used in a paleopole calculation for the unit.

S10: This site contains nine samples from a fine-grained intermediate dyke, all starting with moderate magnetic moments and all demagnetized to magnetite-like unblocking temperatures. Low-temperature fits were made to all samples, along with either MTO or DTO lines. There is a general clustering (seven of nine, the two outliers being samples H and I) of directions in the easterly shallow direction, both in the northern and southern hemispheres (Figure 15). Samples A and B are upward, while the rest are downward, but this changes in the shift to high-temperature directions. The overall azimuthal pattern remains consistent for the high-stability components, with a general drift of components slightly northward. However, now the two upward components are samples B and E. The fact that the low-stability directions are basically the same as the high-stability directions shows that there is a variety of grain sizes and different minerals within the samples. Looking at the path of demagnetization on the orthographic plots, there is a large drop in magnetization between 300 and 350°C, which is indicative of pyrrhotite. These mid-thermal steps were included in least squares analysis for the site. The last two samples, H and I, did not contain this pyrrhotite step. They also both have higher magnetic intensity, a large drop in magnetism at the liquid nitrogen step, and contain only a single component which decays directly to the origin, all of which are evidence of lightning interference at the site. Both of these samples were also collected near the same spot on the outcrop, so it is likely that lightning could have affected that region of the site.

INTERPRETATION: Both the low-stability and high-stability components from this site can be used toward the calculation of a Swartbooisdrif pole taking into consideration the error associated with Fisher statistics in each case. The eastern shallow directions seen in this site are similar to sites S02 and S03 and (maybe) the reverse polarity of site S08. This site is used in the final calculation of a Swartbooisdrif paleopole.

S11: Brown carbonatite was sampled at this site, and all nine samples are demagnetized to magnetite-like unblocking temperatures. Most of the data was very scattered, and decay to the origin always occurred before 570°C, largely due to the fact that a majority of magnetization was removed at the liquid nitrogen step. This substantial jump in magnetization is likely indicative of a greater proportion of multi-domain magnetite in these samples, making the site less reliable than others in the region. Using the same multi-domain ratio calculation spreadsheet as in sites S03 and S04, the samples with the lowest ratios, and thus likely to have the most reliable directions, are A, F, G, and H (but it should be noted that all ratios were very high: 0.75 or higher). This objective

means of sorting out which components to use is necessary in this case, because there is very little consistency in both low-temperature and high-temperature component directions.

The low components for eight of nine samples are in the southern two quadrants, with most lying directly south and shallow. A, G, E, and H are all in this location and directed upward, while F (also upward) lies roughly 90° away to the northeast. The other samples are mostly downward and show no coherent clustering. The high-temperature components, which consist of four DTO fits, three MTO fits, and two SEP fits (for which HPL fits were also made), are mostly in the southwestern quadrant with moderate inclinations, demonstrating a slight shift westward from low to high temperature steps. Again, A, E, G, F, and H are all upward and form the majority of the cluster, none of which are fit to SEP lines. Fisher statistics on this group have sizeable error (a95 = 29.0), and statistics on the low-component directions are even worse (a95 = 33.5).

INTERPRETATION: Although there is a general clustering of both low- and high-stability component directions toward the southern and southwestern shallow directions, there is large error associated with these clusters, which may not make them suitable for contributing to a Swartbooisdrif paleopole. A spreadsheet to calculate multi-domain ratios using magnetic moments at the NRM and LN2 steps was utilized to determine which samples could be considered the most reliable. However, all samples had high ratios, so it is likely that all samples have a large proportion of multi-domain magnetite, contributing to the scattered final directions unsuitable for use in a final paleopole calculation.

S12: This site also contained messy data like the previous, even though all samples begin with moderate magnetic moments and the jumps in magnetic moment from NRM to the LN2 step are not nearly as large as in S11. These nine samples taken from a dark mafic dyke were all demagnetized to 592°C and were fit with LOW and/or MTO lines. Even though orthographic plots were so messy that some samples seemed completely unusable or had only one distinguishable component, there is a general motion from east to west for every sample moving from low- to high-temperatures. All samples except B were fit with a LOW component, and these all lie in the two eastern quadrants, all directed upward besides samples H and I. High-stability components were fit for all samples except H (even though some have high MAD values), and they are all in the two western quadrants in an upward direction. Seven of the eight samples are in the southwestern quadrant, and the one outlier (E) is in the southern part of the northwestern quadrant (Figure 15). The average direction centers on samples A, D, and G in a west-southwestern direction with moderate inclination. It is important to note that some of these samples have fits where the MAD

values are greater than six just because data points are so scattered. Some samples even look to be unusable, especially D, F, and H, so these can and probably should be removed from the final Fisher statistics calculations.

INTERPRETATION: The demagnetization process for these samples was, for some reason, not as straightforward as for other sites. Although there is a general sweep from low-temperature components in the east to high-temperature components in the west, this site may not be reliable. Fisher statistics can be calculated for both LOW and MTO fits, but are associated with significant error. However, including all eight samples, the mean declinations and inclinations and a95 values were similar to eliminating three samples with the highest error. All eight samples were included in the final statistics, and it is obvious the three samples with highest error are being pulled toward the low component. The site is used in the calculation of a preliminary Swartbooisdrif paleopole.

S13: The last site in the Swartbooisdrif region consists of ten samples taken from a dolerite dyke, all of which were demagnetized to 580°C. This is now the fourth site in which the decrease in magnetic moment from the NRM step to the LN2 step is relatively large, suggesting greater proportions of multi-domain magnetite. Multi-domain ratios were calculated for all sites, showing that samples D, G, H, I, and J are the five that can be considered most reliable since they have the smallest ratios. All ratios were relatively high, though (0.75 or higher), so it is almost certain that multi-domain magnetite makes a contribution throughout the site. All samples were fit with both LOW and MTO lines, and there is a general motion of all samples from north to south going from low to high temperatures.

The low-stability components are all in the northern two quadrants, generally in a northerly very shallow direction. Five samples in this direction are downward and four are upward, while the final sample (E) is an outlier in an east-northeasterly shallow upward direction. Approaching high-temperatures, all samples shift toward the southwest, moving along the edge of the stereonet. All high-stability components lie in a southwesterly shallow direction with the exception of three (C, F, H) which lie west-northwesterly and shallow. All are upward except for two (B, F), and Fisher statistics are calculated to contribute to a paleopole (Figure 15).

INTERPRETATION: A large portion of magnetic moment is lost at the liquid nitrogen step for all samples in this site, which indicates a greater proportion of multi-domain magnetite than in other Swartbooisdrif dolerite dykes. The direction of high-stability components is similar to the mean direction in sites S08 and S12, but different from S02, S03, and S10 (close to reverse polarity, but not quite). The high-temperature component directions are be used in the calculation of a

Swartbooisdrif pole. It also should be noted that the low component is indicative of the Cenozoic local field (Torsvik, et al., 2012).

In order to create a more complete Swartbooisdrif paleopole, we augmented our dataset by including data from three north-trending dykes from Angola. The samples were collected by Johanna Salminen, and we include the data from three sites in our preliminary Swartbooisdrif pole (Johanna Salminene, personal communication, March 2015).

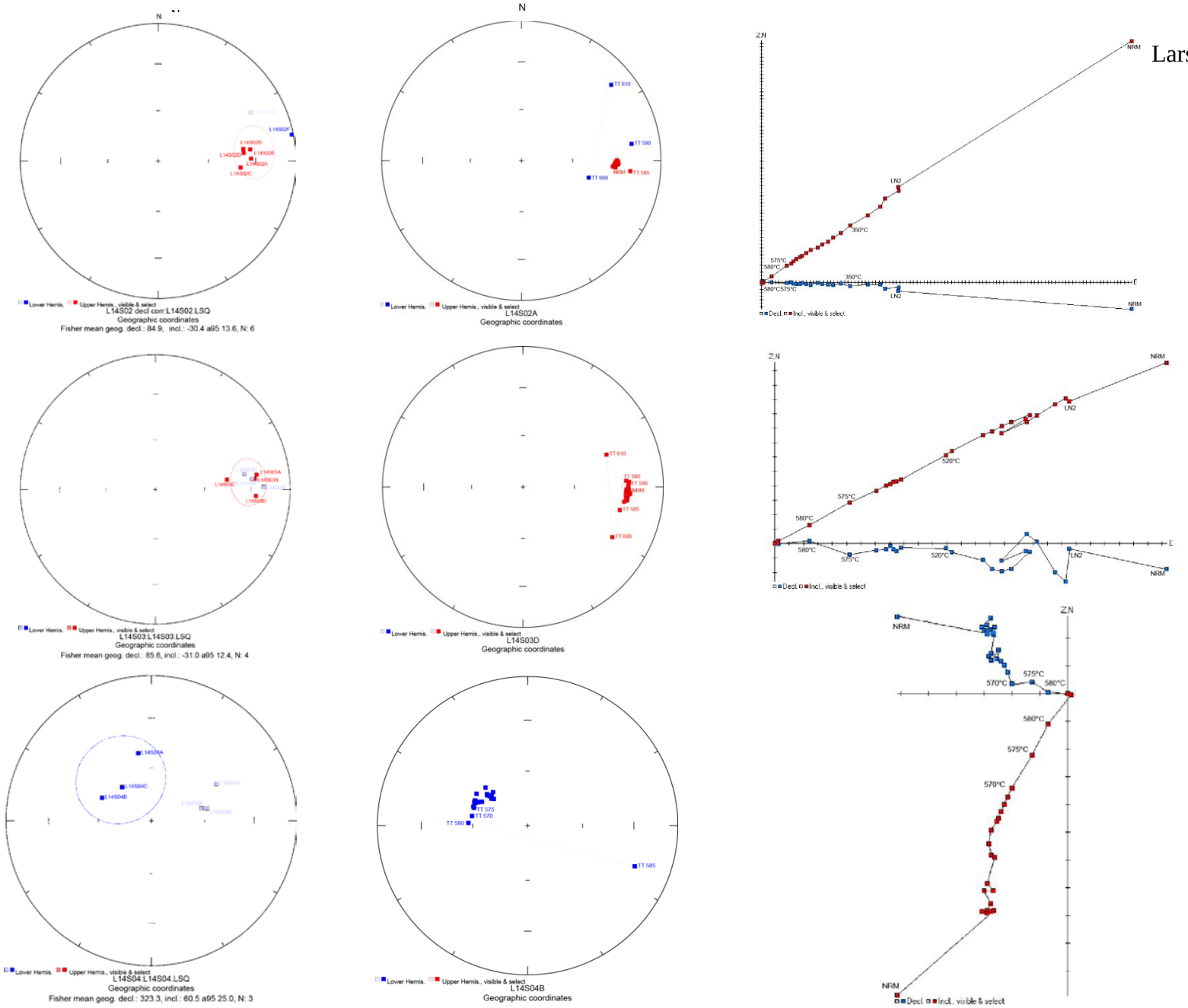

Figure 14: Sites L14S02 (top row), L14S03 (middle row), and L14S04 (bottom row) demonstrate a positive baked contact test. The dyke (S02) and anorthosite it intrudes (S03) possess the same high-temperature component direction and also have similar equal area and orthographic plots, suggesting that the surrounding rock was remagnetized by the dyke. In anorthosite further from the dyke (S04) this mean direction changes significantly.

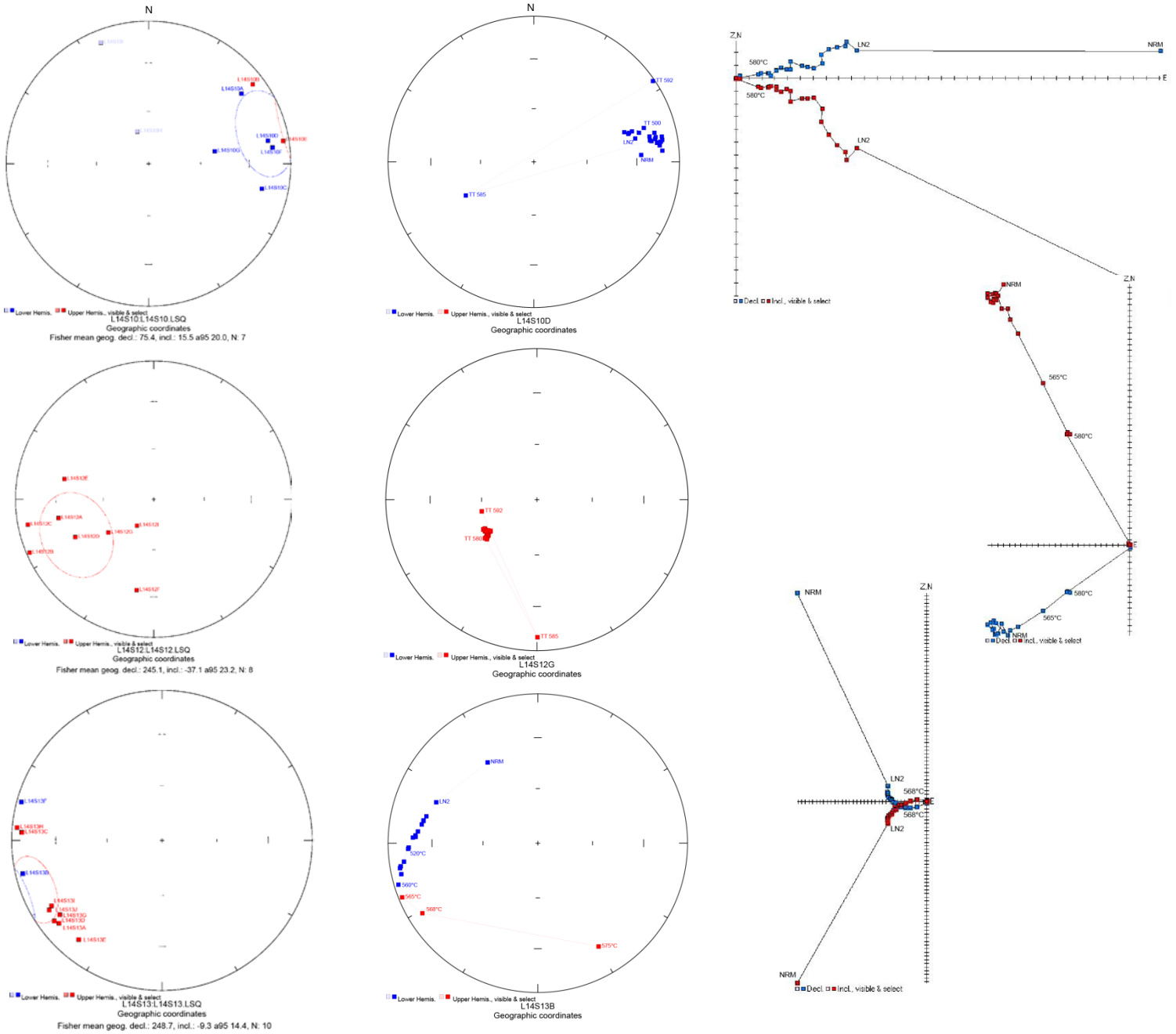

Figure 15: Sites L14S10, L14S12, and L14S13 (from top to bottom) were also used in the calculation of a preliminary Swartbooisdrif paleopole. From left to right is each site's high-stability mean direction with a Fisher statistics error ellipse, equal area stereonet for a representative sample from the site, and the corresponding orthographic Zijderveld plot for those samples.

Epembe Syenites

Seven sites were sampled from the Epembe area, four of which provide data contributing to a mean direction for the unit. Data plots for these sites are shown in figures 16 and 17.

E01: Seven samples are taken from this unit where amphibolite basement rock is intruded by apophyses of epidote-altered nepheline syenite. All samples in this site are nepheline syenite, while the basement rock is sampled as site E02. Lack of layering within the site implies no tilt correction, and the demagnetization behavior between all samples is messy. However, four of the seven samples give a final magnetic (ChRM) component in a generally southern, high inclination, downward direction (Figure 16). Magnetic moment is moderate amongst all samples (usually beginning at 1e-04 or 1e-05 emu), yet only two samples were completely demagnetized by 585°C (A and E). The rest contained a hematite component, which decayed directly toward the origin (HTO in LSQ files) after a low component was removed predominantly below ~300°C, although rarely between 300 and 350°C.

The high temperature components for this site are not tightly clustered, but do fall mostly within the southwestern quadrant. However, they are a bit steeper in inclination and all downward. No apparent patterns emerge between these directions and whether or not demagnetization occurred at magnetite vs. hematite levels. A low-thermal component was noted in sample G, which resembles the low components for the other samples. Planes were fit for sample E after a mid-thermal component was determined. This mid-thermal component (MTH) is very similar to the mid-thermal component found in sample A, but both are ~90° away from the mid-thermal component of sample D. The two high plane (HPL) fits to E contain different sets of points (HPL fits just to the points in the MTH component, which HP2 fits the MTH components plus the high temperature steps—to 585°) but are very similar.

INTERPRETATION: This site contains a primary shallow SW-up magnetic component in low unblocking-temperature minerals, which is surprising since this is the direction of high temperature ChRM components for three of seven Epembe sites—the direction is consistent amongst all samples in those three sites, which provides good Fisher statistics for a preliminary Epembe paleopole. Although it might be tempting to use this component in the calculation of an overall mean direction of presumably primary age for the Epembe complex, the low unblocking temperature would be rare for preserving Mesoproterozoic remanence. Still, 300°C corresponds to prehnite-pumpellyite regional metamorphic facies, and widespread preservation of primary olivine and pyroxene in the host Kunene Anorthosite complex (Maier et al., 2013) suggests that the

regional metamorphism was indeed very low. Thus, the low-temperature component is included in the overall mean paleomagnetic pole for the Epembe complex.

E02: This site consists of the amphibolite basement rocks in the Epembe unit which are intruded by veins of nepheline syenite. The amphibolite is extremely friable, so only five samples were collected successfully. Because of the samples' tendency to physically disaggregate, the highest temperature step reached was 450°, after which all samples had crumbled into pieces not suitable for measurement on the magnetometer. Since all five samples provided messy, inconclusive data (scattered across stereonet, extremely weakly magnetized with three of five samples with intensity on the order of 1e-07 emu), the least squares will not be used in principle component analysis for Epembe. Because of this, these early Mesoproterozoic amphibolite host rocks (Seth et al., 2003) of the Epembe syenite proved unsuitable for paleomagnetic analysis.

INTERPRETATION: Amphibolite host rocks (early Mesoproterozoic; Seth et al., 2003) of the Epembe syenite proved unsuitable for paleomagnetic analysis.

E03: This site samples more of the Epembe nepheline syenite, but, in this locality, layering provides a tilt-correction for the site. Seven samples were collected: the first four are medium-grained while the other three are coarse-grained. All begin with magnetic moments of ~1e-04 or ~1e-05 emu, and four sites show a consistent high temperature component directed to the south with moderately upward inclination. All samples were completely demagnetized before 580°C, suggesting pure magnetite unblocking (no hematite component). Although the ChRM direction is tightly clustered for these four samples (C, E, F, G), there are two major outliers (A and B), which have high temperature components in the west-southwest, shallow, upward and north-northeast, shallow, upward directions, respectively. Intensity plots (J/J0) for these outliers do not suggest lightning interference—the plots show a clear magnetite component being removed (quicker toward higher temperatures) and are similar to intensity plots for the rest of the samples in the site. Sample D was completely demagnetized by 560°, so a low-unblocking temperature component was determined but no stable endpoint or decay to origin was observed. In total, four low-unblocking components were determined from the site, three of which are easterly and steep upward. Two high planes were also fit (samples B and C), but since the data points (demagnetization steps) were so scattered, produce no clear decay toward the origin or a stable endpoint.

INTERPRETATION: The south-upward directed, high-stability component yields a virtual geomagnetic pole similar to Early-Middle Cambrian south poles for Gondwana (Mitchell et al.,

2010) and is tentatively interpreted as an overprint related to late stages of the Pan-African orogeny in Kaokoland. Therefore, this site is not included in the calculation of an Epembe paleopole.

E04: All of the samples in this site displayed pure magnetite-like unblocking temperatures, with complete demagnetization occurring by 585°C for all samples. Like E01, these seven samples are nepheline syenite with no apparent layering. They begin with stronger magnetic moments (1e-03 or 1e-04 emu) than the previous sites, and all give downward ChRM directions. While the downward polarity is consistent across all samples, the inclination and declination values have greater variance. Four samples have a north or northwestern azimuth (A, B, F, G), while the other three are in the general southwestern direction, with inclination values ranging from very shallow to very steep. Five low-temperature components were defined during least squares analysis, and these again lie mostly in the southwestern quadrant, but, unlike other Epembe sites, are predominantly downward. Only one component (from sample B) is upward-directed, and it lies in an eastern shallow direction. Three (C, D, E) are southwesterly and shallow, while the last (G) has an unusual south-southeastern steep downward direction. Fisher statistics were not used for the low or high component data in this site due to the large spread in directions. It might also be important to note that two mid-thermal components were recorded in the site (samples B and C), but there is no pattern or significance in these directions (northeastern shallow downward and southeastern steep downward).

INTERPRETATION: In sum, the coarse nepheline syenite at this locality yielded only scattered remanence components, unusable for calculating a paleomagnetic pole.

E05: This site produced consistent ChRM directions amongst all seven samples. Each sample, taken from dark mafic rocks, starts with a strong magnetic moment (~1e-02 emu) and demagnetizes around a hematite unblocking temperature (by 685°). Closer examination of the intensity plots (J/J0) for these samples reveals a second component with a significant jump in demagnetization occurring around magnetite-like unblocking temperatures, suggesting a magnetite imprint throughout the site. Five of the seven samples have a low or low-thermal component, the difference between the two being the number of steps used in the projection of a line in least squares analysis. A low component will be made up of only the first two to four steps, while a thermal component is defined by more steps (up to 450° in sample E05G). These five low components are all clustered in a generally southern, shallow, upward direction (there is some spread from east to west).

The high-temperature components were all fit as hematite-to-origin (HTO) decay lines—the orthographic projections are nearly perfectly linear and the fits all have errors (MAD) under 5.0. Six of the seven high temperature components share the west-southwest, shallow, upward direction, which is later seen in sites E06 and E07 (Figure 16). The seventh sample (F) has a south-southeast, steep, upward direction, and is excluded from the site's Fisher statistics. The NRM moment (~9e-02 emu) is nearly double that of the next strongest sample from this site, and this attribute plus substantial unblocking at low demagnetization levels suggest the influence of lightning at that location on the outcrop. Higher demagnetization levels in this sample show drift of the directions toward the SW quadrant, but no linear fit of the ultimate component is possible.

INTERPRETATION: The low-stability component yields a virtual geomagnetic pole within error of the Early-Middle Cambrian APWP for Gondwana (Mitchell et al., 2010) and could arise from partial magnetic overprinting of that age, associated with the Pan-African orogeny in Kaokoland. The high-stability component appears to be held by both stoichiometric magnetite and hematite, and likely results from a primary thermal-remanent magnetization (TRM) and subsequent deuteric alteration (crystallization-remanent magnetization; CRM) upon intrusion of the mafic dyke at shallow crustal levels. This site is used in the calculation of an Epembe paleopole.

E06: Demagnetization trends similar to those in E05 are seen in the seven samples in E06. However, there is no consistent low component in the site. This site consists of dark gray-green mafic rock—the first two samples are coarse-grained, while the rest are finer-grained. This may be important in how the high-temperature component is preserved in the rock. Looking at the ChRM directions, all five finer-grained samples are clustered tightly in an easterly shallow upward direction. The two coarser-grained samples are also upward, but they are slightly north and east of the main cluster, creating almost a mirror image of the main cluster offset to the northeast. In terms of magnetic moment, though, the coarser-grained samples (A and B) start out at a similar level as the finer-grained samples (~1e-03 emu), so lightning is not expected to be the cause of this discrepancy. Both A and B reach complete demagnetization at 665°C, so a hematite-like component is most likely present. Looking at the intensity plots for these two samples, most unblocking actually occurs at a magnetite-like unblocking temperature, which makes it clear that there are two components in these coarser-grained samples and demagnetization predominantly occurs in the magnetite temperature range. Four of the other samples (C, D, F, G) are single-component, with one drop in magnetic intensity happening around a magnetite-like unblocking temperature. There is one anomaly—sample E is not completely demagnetized until 665°C but the

intensity plot shows no evidence of a magnetite component. There is one very steep drop in intensity at a hematite-like unblocking temperature. Also, the high-temperature component for sample E is downward rather than upward even though it correlates in inclination and azimuthal direction with the other samples. This sample does begin with a weaker magnetic moment (~1e-05 emu), but sample F also begins with a weaker moment yet does not have this anomalous downward direction.

This "bimodal" inconsistency is interesting to note, because it shows up in both the low and high temperature components. Although there is no consistency amongst the low-temperature component directions (broad scatter across the stereonet), they are still split 3-and-3 between the northern and southern hemispheres, creating a mirror image, with one anomaly (E) pointing downward. Perhaps this suggests that some sort of systematic error was made with E. The high temperature fits are clustered more tightly, so the "bimodal" distribution is not as extreme, but there are still points in both the northern and southern hemisphere, all in an upward direction. Fisher statistics are calculated for the high temperature ChRM components excluding sample E, which are all easterly and shallow upward, and this is used in the calculation of the preliminary Epembe pole (Figure 17).

INTERPRETATION: While the low-stability components are not reliable for this site, the high-temperature components mostly cluster in an easterly shallow upward direction, providing good Fisher statistics, so the site is included in the final paleopole calculation for the unit. This site does have one outlier, but this sample is excluded in principle component analysis so that a virtual geomagnetic pole can be created. Interesting correlations between grain size and unblocking temperatures are made, and an unusual "bimodal" distribution in both high- and low-temperature components brings up questions of systematic error.

E07: This site is made up of eight samples from a northwest-striking dolerite dyke which intrudes a northeast-striking gneiss. Samples are taken within 50 centimeters of the contact, with E and F being furthest away. The dyke is at least 100 meters wide, and the dolerite becomes gabbro (medium-grained) several decimeters from the contact. All samples begin with moderate magnetic moments around 1e-04 emu and mostly follow the same demagnetization pattern. The low components from all eight samples are upward, but follow a "bimodal" distribution similar to the one in E06, where half of the samples (A, B, E, F) have low-stability components that are southwesterly and very steep and the other half (C, D, G, H) have low-stability components that are northeasterly and shallower. The high temperature ChRM components are much more consistent

throughout the site, though, and do not produce this “bimodal” distribution. All samples were demagnetized through a magnetite-like unblocking temperature (580°C) and produce single-component magnetite-to-origin (MTO) decay lines with very little error (all below MAD 6.0). Intensity plots for all samples confirm the single-component demagnetization of these samples and suggest no lightning interference at the site. These form a tight cluster in the southwestern shallow upward direction, which gives reliable Fisher statistics to be used in the calculation of the preliminary Epembe paleopole (Figure 17).

INTERPRETATION: The “bimodal” distribution seen in low-stability component azimuths may have something to do with distance from each sample to the dyke contact, but there seems to be no obvious pattern when checking over field notes. Samples G and H are north of A and B, and both are in the cluster in a northeastern steep upward direction. E and F are furthest from the dyke contact, and they are both in the second cluster. From this, it could be possible that the intrusion of the dyke affected the magnetism in the samples closest to the contact. While these low-temperature components cannot be used to create a paleopole, the high-stability components provide high-quality Fisher statistics and will be used in combination with E05 and E06 to calculate a preliminary Epembe paleopole.

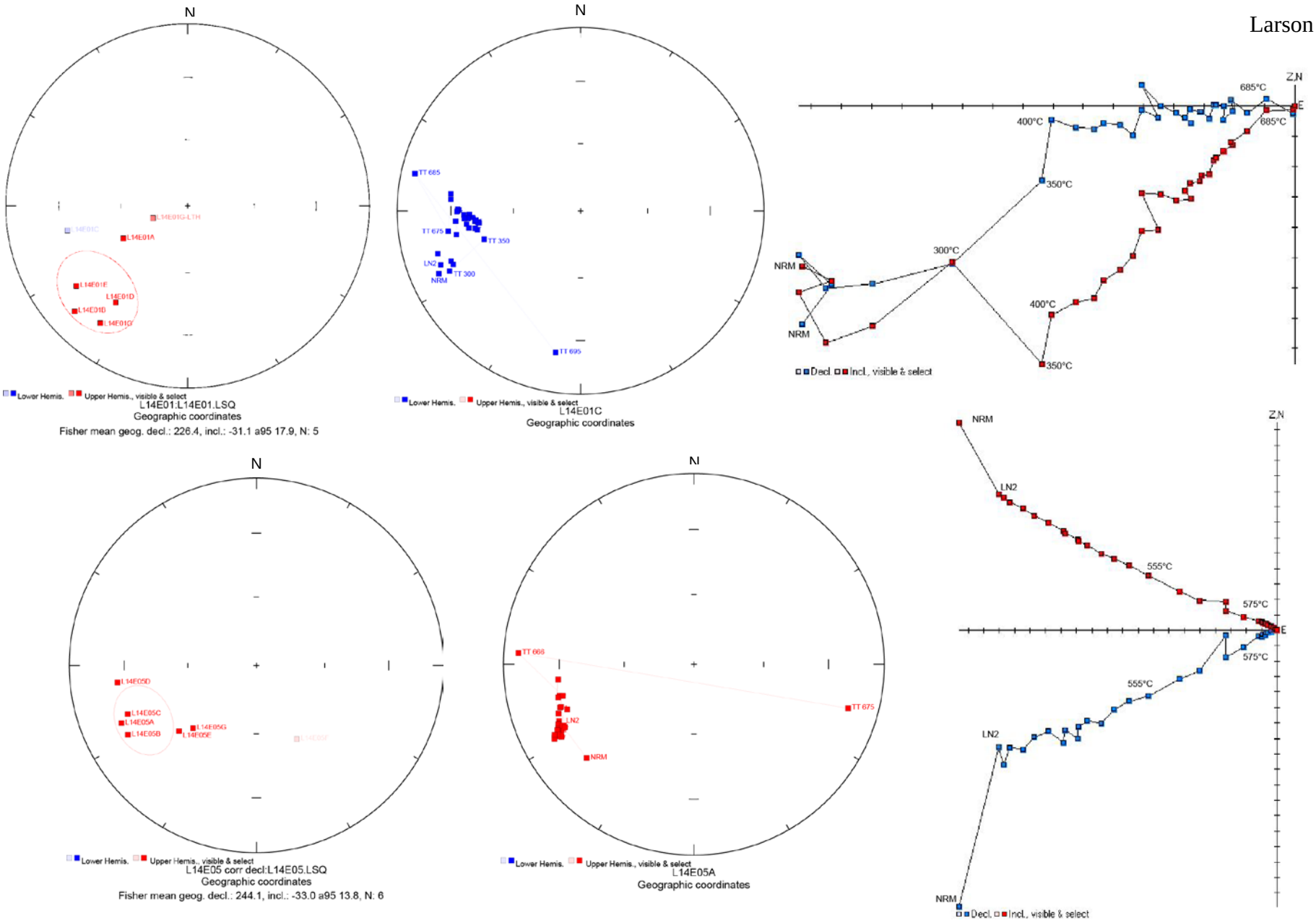

Figure 16: Four of seven sites were used in the calculation of the preliminary Epembe paleopole, the first two of which are L14E01 and L14E05. In the top row, from left to right, is the mean low-stability component direction with Fisher statistics error ellipse, equal area stereonet, and orthographic Zijderveld for L14E01. The same three plots are shown in the row below for L14E05.

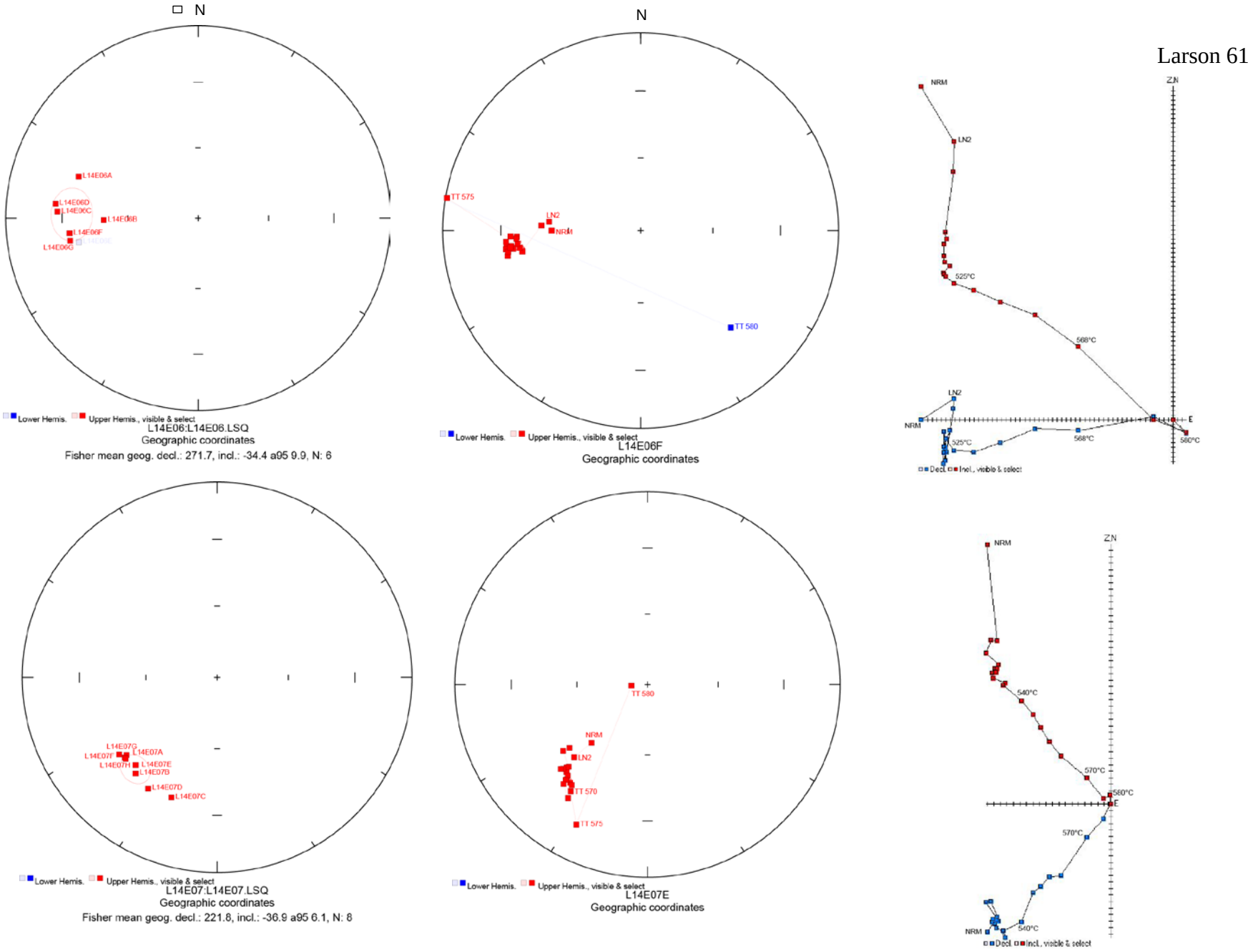

Figure 17: The second half of the sites used in the calculation of the preliminary Epembe paleopole are L14E06 and L14E07. In the top row, from left to right, is the mean low-stability component direction with Fisher statistics error ellipse, equal area stereonet, and orthographic Zijderveld for L14E06. The same three plots are shown in the row below for L14E07

DISCUSSION

From this project, three new preliminary paleopoles have been produced and can be added to the database of Meso-Neoproterozoic Congo-SF poles after further sampling. Using four of seven sites, we calculate a preliminary mean Epembe paleopole at 19.7°S, 105.6°W with statistical precision K = 14.5 and A_{95} = 24.9. Using six of thirteen sites (site S08 is included in this pole to increase N value, but can be removed for better precision without significant change to the overall direction), and the supplementary three sites from Angola (Salminen, personal communication, March 2015) we calculate a preliminary mean paleopole for Swartbooisdrif at 20.1°S, 86.5°W with statistical precision K = 16.9 and A_{95} = 12.9. Last, using the 75% unfolded data for the five most reliable Kunene sites (L14S04, L14K06, L14K07, L14K13, and L14K14), we calculate a preliminary mean Kunene paleopole at 40.2°N, 131.4°W with statistical precision K = 17.5 and A_{95} = 18.8.

Using these poles, the relative locations of the Congo-SF and Kalahari cratons are analyzed from the Mesoproterozoic into the Neoproterozoic to produce models of possible Nuna configurations. Before creating these reconstructions, two field stability tests were completed in order to ensure the validity of the data presented here. A baked contact test was confirmed positive using three sites in the Swartbooisdrif unit. Nest, a conglomerate test using two sites from the Kunene unit is determined positive. Finally, in addition to the stability tests, a fold test for the Kunene unit is performed in order to account for the doming of the anorthosite complex at the time of magnetization. Although these tests confirm the reliability of the sites chosen for analysis, increasing the number of sites at each of these localities will be essential in improving the range of error, and also in supporting the conclusions suggested below.

Using the 38 sites presented in this thesis, three different null hypotheses on the enigmatic relationship between the Congo-SF and Kalahari cratons are tested and discussed. Using GPlates software, the two most reliable poles from Swartbooisdrif and Epembe are compared to poles from the Kalahari craton of approximately the same age. Three different proposals on where Congo-SF and Kalahari could have been located during the formation and subsequent breakup of Nuna are suggested, each of which with a different level of likeliness for occurrence. Geological processes are taken into account in these discussions, where matching geological features on each craton are utilized to reposition the cratons in relation to each other. As previously stated, the ideas presented here cannot be confirmed until more data is obtained, but these hypotheses lay the groundwork for

further research. Additional sampling of the Kunene Complex along with the satellite Swartbooisdrif and Epembe regions should be the next step in moving this research forward.

Swartbooisdrif Baked Contact Test

Sites L14S02, L14S03, and L14S04 provide evidence of a positive baked contact test (Figure 11). L14S02 contains samples from a syenitic dyke, which seems to intrude the massive anorthosite of L14S03. Site L14S04 contains samples of anorthosite taken a further distance from the contact, which provides demagnetization component directions used in comparison with the anorthosite of L14S03. If the syenite dyke of L14S02 intruded L14S03 and remagnetized the rock in direct contact with it, we expect the two sites to share the same high-stability direction of magnetization. The stable country rock should hold a remanent direction that is different from the dyke and direct contact if it was not remagnetized by the dyke intrusion. In this case, sites L14S02 and L14S03 exhibit the same high-stability component direction (easterly and shallow upward), while L14S04 has a high-stability direction in an entirely different direction (northwesterly and steep downward). From this, it is clear that the dyke in L14S02 intruded and remagnetized the anorthosite in close contact. It should also be noted that, since the anorthosite in L14S04 has a different high-stability direction, the entire unit as a whole has not been remagnetized since the time of the dyke intrusion.

Kunene Conglomerate Test

Sites L14K12F and L14K12M are both taken from the same conglomerate unit along the southwestern margin of the Zebra Mountains. According to the Swartbooisdrif 2002 Geological Survey Map used to create Figure 4, this outcrop is classified as part of the Nosib Group (Schreiber, 2002, compiler). The Nosib Group has a suggested age of 750 Ma or older, with the potential of being as old as Mesoproterozoic (Hoffman and Halverson, 2008; Hoffman 2011). However, Hedberg produced a geological map which shows the L14K12 outcrop as part of the Mulden group (Hedberg, 1979). The Mulden group lies atop the Damara succession in northern Namibia, and is dated to be Ediacaran to possibly Cambrian in age. Since this discrepancy in age of the conglomerate unit exists, the positive conglomerate test presented here has no specific implications for the sites collected in the area.

In Figure 9, the data from both L14K12F and L14K12M is presented, revealing no consistent high-stability component direction within each site. Samples were collected from both felsic (L14K12F) and mafic (L14K12M) cobbles within the conglomerate, and some cobbles were sampled twice. If the cobbles were magnetized before the conglomerate unit formed, we expect that

each cobble will give different directions of magnetization. However, if the entire unit has been remagnetized, all cobbles would maintain a similar direction of magnetism. Since the first situation is true in this case, these two sites provide a positive conglomerate test for the region, proving that the rocks have not been remagnetized since the time of the conglomerate formation (which is unknown). Also, we show that the data from L14K12F is more reliable than the data of L14K12M, since samples from within the same cobble produce the same high-stability direction. In L14K12M, there are differences in directions within cobbles, which are unexpected and could indicate systematic error throughout the site. This renders L14K12M obsolete in proving a positive conglomerate test.

Kunene Fold Test

Kunene region samples were taken from sites which follow the outer margin of the Zebra Mountain Lobe. Although demonstrable tilt correction was collected at each site, a partial fold test was performed to find the point of maximum site mean clustering (Figure 18). The Zebra Mountain Lobe is presumed to have been created by a large mantle upwelling, which had a doming effect on the overlying lithosphere to create the large Kunene anorthosite massif (Maier, et al., 2013). Because of this, we consider Kunene paleomagnetic remanence to be acquired during the medial stages of the doming process. In order to determine the point of folding at which remanent magnetization was most likely locked into these rocks, Fisher's precision parameter was calculated for all levels of unfolding (Fisher, 1953). This fold test is significant at over 95% confidence between the 0% and 75% levels of unfolding. More precisely, the null hypothesis that K is the same at 0% and 75% is rejected with greater than 99% confidence (Fisher, 1987, p. 219). This high level of confidence also applies to the interval 0% to 100%, where the null hypothesis can be rejected with 90-95% confidence. Between 75% and 100%, the null hypothesis is only rejected with 60-65% confidence, but this uncertainty is not substantial enough to diminish the results of the fold test. In Figure 16, mean directions from the five most reliable sites are shown plotted together on equal-area stereonets. As folding approaches the 75% level, clustering of these means becomes tightest before they once again diverge nearing 100% folded. This suggests that the remanent high-stability component of magnetization was locked in while the unit was still folding.

Using the 75% unfolded data for the five most reliable sites (L14S04, L14K06, L14K07, L14K13, and L14K14), we calculate a preliminary mean Kunene paleopole at 40.2°N, 131.4°W with statistical precision $K = 17.5$ and $A_{95} = 18.8$. This paleopole is substantially different than the pole reported by Piper in 1974. Piper sampled the complex to the north in Angola, then, using

alternating-field demagnetization, he produced a pole at 3°S, 255°S with a low statistical precision K = 7. He states that this low precision is likely caused by apparent polar wander during the time of cooling. Since his study utilized outdated methods to produce data with such low precision, further comparison with our pole is inconsequential.

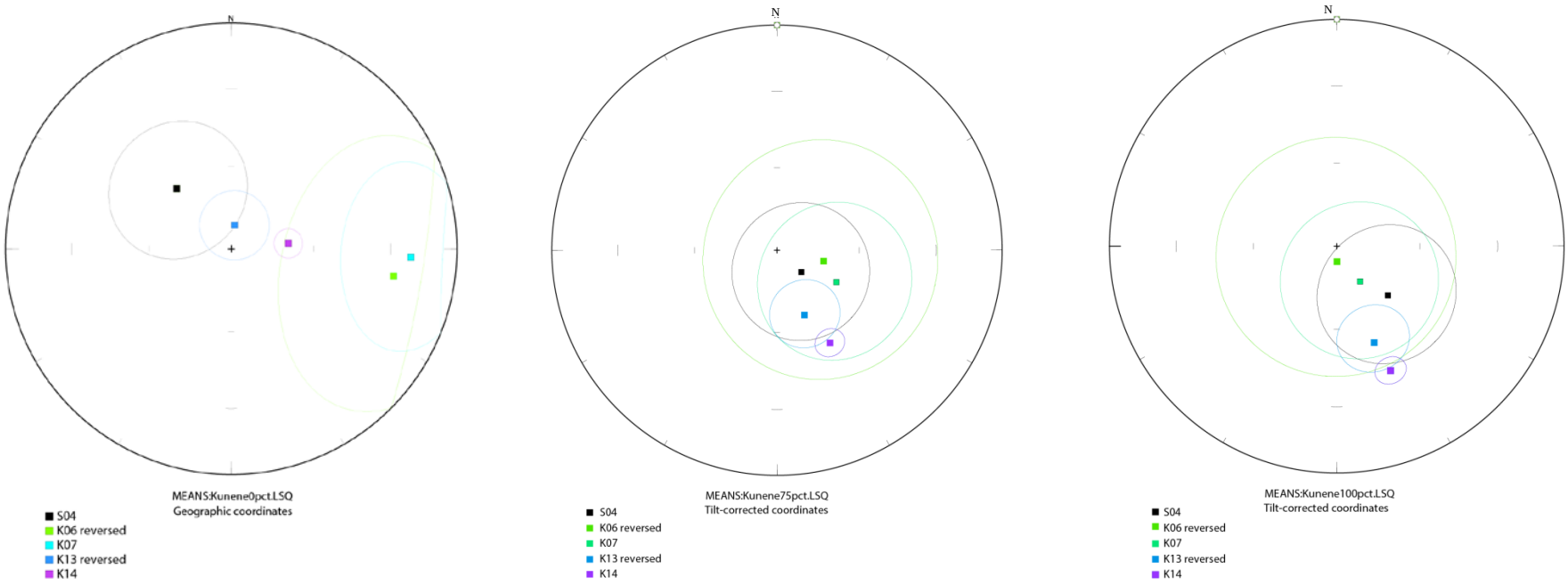

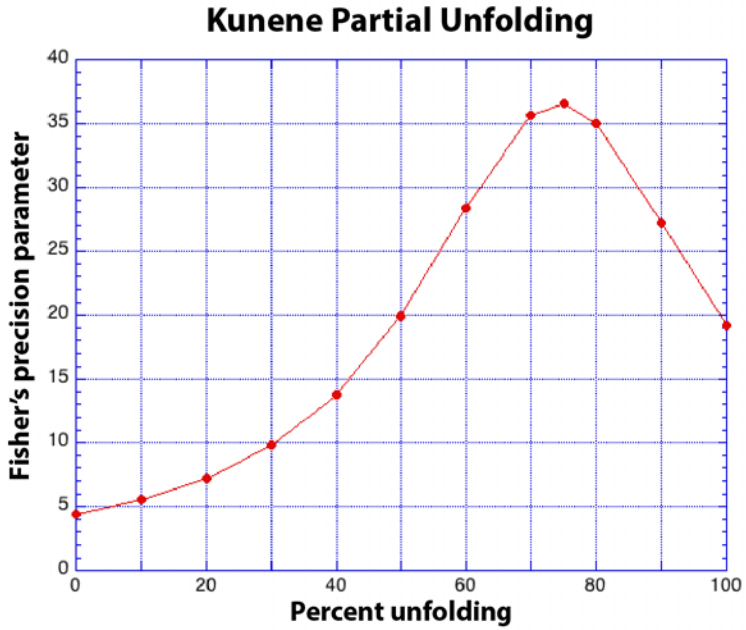

Figure 18: Although sampling in the Kunene region provided demonstrable tilt correction, partial unfolding is necessary to see maximum clustering amongst site mean directions. Beginning without any tilt correction (top row, far left), clustering of site means is maximized around 75% unfolding (top center) before precision begins to drop closer to 100% unfolded (top, far right). The chart below these stereonets shows how well site means converge through Fisher's precision parameter in terms of percent unfolding.

Configurations Relative to Supercontinent Nuna

In our reconstructions, we focus mainly on the relative locations of Congo-SF and the Kalahari craton. The two most reliable preliminary paleopoles derived here can be compared to poles of nearly the same ages for Kalahari in order to examine the relation between the two cratons. The third pole we derive (Kunene) can also be compared to a mean pole we have calculated from a collection of poles published by Gose, et al. in 2013, which we call the Kalahari Alkaline Mean. However, due to the large error in both of these poles, our reconstructions are not based on their correlations, but rather just shown for comparison. The Swartbooisdrif pole at 1130 Ma can be correlated with the well-defined 1110 Ma Umkondo pole from Kalahari (Gose, et al., 2006; 2013). Additionally, our Epembe pole at 1210 Ma is most directly comparable to the Premier Kimberlite pole, which was originally dated at around 1215 Ma (Doppelhammer and Hargraves, 1994). However, only recently, a new age for the Premier Kimberlite suggests the unit is closer to 1150 Ma (Wu, 2013). This pole, while not within error of the age of the Epembe pole, still provides a reference for the movement of Congo-SF and Kalahari through time. With this set of four poles, three new hypotheses are proposed for configurations of the cratons at the time of Nuna buildup. These hypotheses test whether or not the two cratons existed on the same tectonic plate, while also accounting for geological evidence used to support or disprove proposed Nuna configurations.

1. APW Optimized: Kalahari Separate from Congo-SF on Same Plate

In order to optimize the overlap of late Meoproterozoic paleopoles from Kalahari and Congo-SF, the first hypothesis proposes that the two cratons are part of the same plate between 1215 Ma and 1110 Ma but are separated by a substantial distance (Figure 20). Congo-SF remains close to Nuna at this time, again making use of Salminen's 1505 Ma dykes pole which matches the apparent polar wander path for Laurentia, Baltica, and Siberia, while Kalahari is located far from the supercontinent. Our preliminary paleopoles line up sequentially with the poles going from the oldest (Epembe) through the youngest (Umkondo) within error. Even though this configuration optimizes the pole positions, the great distance between Kalahari and Congo-SF suggests that there may be a "mystery" craton that was situated between the two cratons at this time. Assuming this vast area was not oceanic, a third craton that is either yet to be identified or may have subsequently been destroyed as the two cratons eventually merged together must have existed. This hypothesis also does not address the geological issue of sourcing the Swartbooisdrif dykes. While we optimize the overlap of our Congo-SF poles with Kalahari poles of nearly the same age, this is not the ideal way to incorporate the Swartbooisdrif dykes into the Umkondo large igneous province

2. Closest Approach: Kalahari Closer to Congo-SF on Same Plate

Next, we test the null hypothesis that both Congo-SF and Kalahari are close together, in their present-day locations relative to each other. By placing the cratons in their present-day arrangement, it becomes clear that this option is not supported by the paleomagnetic data (Figure 19). The two older poles (Epembe and Premier) overlap within error, but the younger poles are significantly distant from each other, meaning Congo-SF and Kalahari could not have been in this arrangement during the time period we're focusing on. Knowing that the two must have been positioned differently than they are today, we used GPlates to position the cratons in a way that allows them to be both on the same plate and near each other. By rotating the craton around the pole positions from the first hypothesis, this model permits a solution where Congo-SF and Kalahari were near each other between 1215 and 1110 Ma, as the paleopoles are still within error of each other (Figure 21). By keeping Kalahari outside of Nuna, this configuration follows many models in the literature in which Kalahari has an unknown location and is not a central piece of the supercontinent (cite). However, by placing Kalahari on this side of Congo-SF, the source of the Swartbooisdrif dykes and possible linkage to Umkondo magmatism are not explained. Geologically, there is no evidence for a collision of Kalahari and Congo-SF in this formation. The Namaqua-Natal belt along the southeastern margin of the Kalahri craton does not correlate chronologically with any orogeny on the northwestern margin of the Congo-SF craton (cite). Because of this and the fact that we must eliminate the possibility of these Mesoproterozoic dyke intrusions being traced back to the Umkondo large igneous province, this model is less optimal than the first.

3. Integrative Solution: Kalahari and Congo-SF Umkondo Connection

The next hypothesis proposes a slightly inferior fit of Congo-SF and Kalahari paleopoles by stretching plausible craton rotations to the limit in order to consider an arrangement nearly opposite of the second hypothesis. In this situation, Congo-SF and Kalahari come together during the buildup of supercontinent Nuna, and Kalahari is located on the other side of Congo-SF, closer to Baltica and Laurentia. A paleopole from Congo-SF dykes dated at 1505 Ma is compared to the apparent polar wander path for Laurentia, Baltica, and Siberia (Salminen, et al., in prep), allowing for a tighter fit of Congo-SF to the rest of Nuna and suggesting the assembly of the supercontinent around this time. In order to place Kalahari within Nuna, we rotate the craton so that the Congo-SF and Kalahari paleopoles are still within error of each other and Kalahari fits between Congo-SF and Baltica/Siberia (Figure 22). This tight fit capitalizes on the relative location and proximity of the

Swartbooisdrif dykes and the Umkondo large igneous province (LIP). Here, the dykes point directly toward the LIP, which would provide an explanation for the source of the dyke intrusions. With a focus primarily on Congo-SF and Kalahari, this option seems to be the best fit geologically. If this relative position of Congo and Kalahari persisted through Rodinia assembly and breakup, the Damaran evolution between the two cratons would be comparable to the evolution of the Pyrenees in the Cretaceous (Vissers and Meijer, 2012). However, when considering the rest of Nuna, there is neither 1505 Ma nor 1370 Ma magmatism known from Kalahari, which makes it difficult to make geological connections with Laurentia, Siberia, and Baltica. A further investigation into whether this configuration could have persisted into the Neoproterozoic should be the next step in testing the reliability of this model.

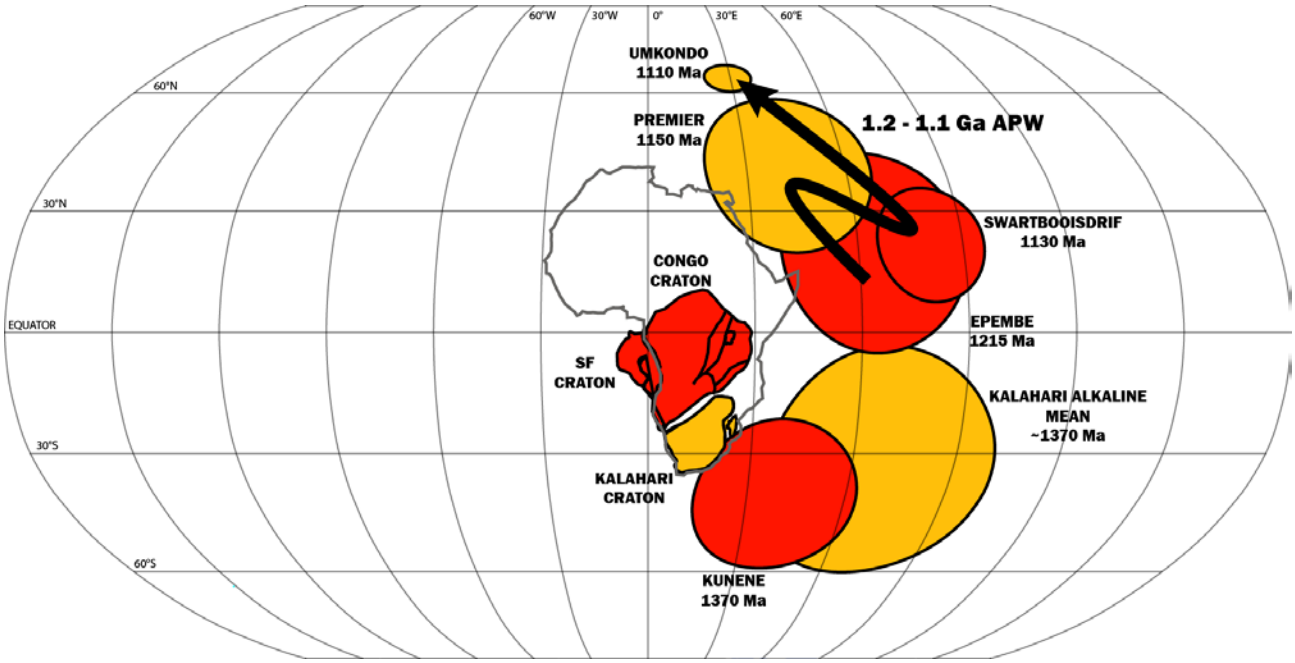

Figure 19: In order to test whether or not Congo-SF and Kalahari could have been situated in their modern-day arrangements during the Mesoproterozoic, the cratons are placed in their current reference frames and paleopoles are compared. Although all poles are in general proximity, the implied joint apparent polar wander (APW) path is rather sinuous, demonstrating the unlikeliness that these cratons were in this static position between 1215 and 1110 Ma.

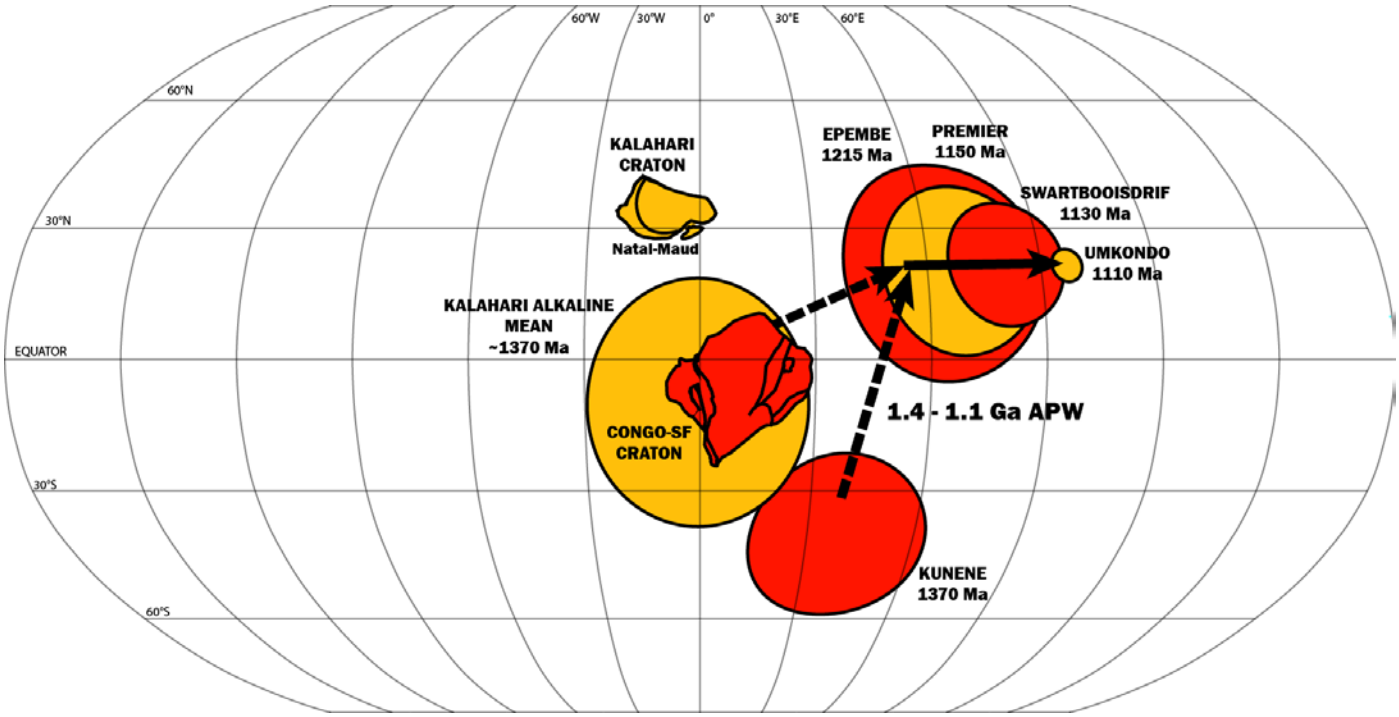

Figure 20: Optimized APW path for the 1.2-1.1 Ga interval, shown in present Congo coordinates. Kalahari and its late Mesoproterozoic poles are rotated by Euler parameters (17.3°N, 056.0°E, -86.3°). The 1370 Ma poles do not overlap in this reconstruction, implying that the hypothesized assemblage formed between 1370 and 1215 Ma, likely via oblique collision along the Natal-Maud orogen. If the two cratons are on the same plate at this time, the question of whether or not a third, unknown craton lies between them is posed.

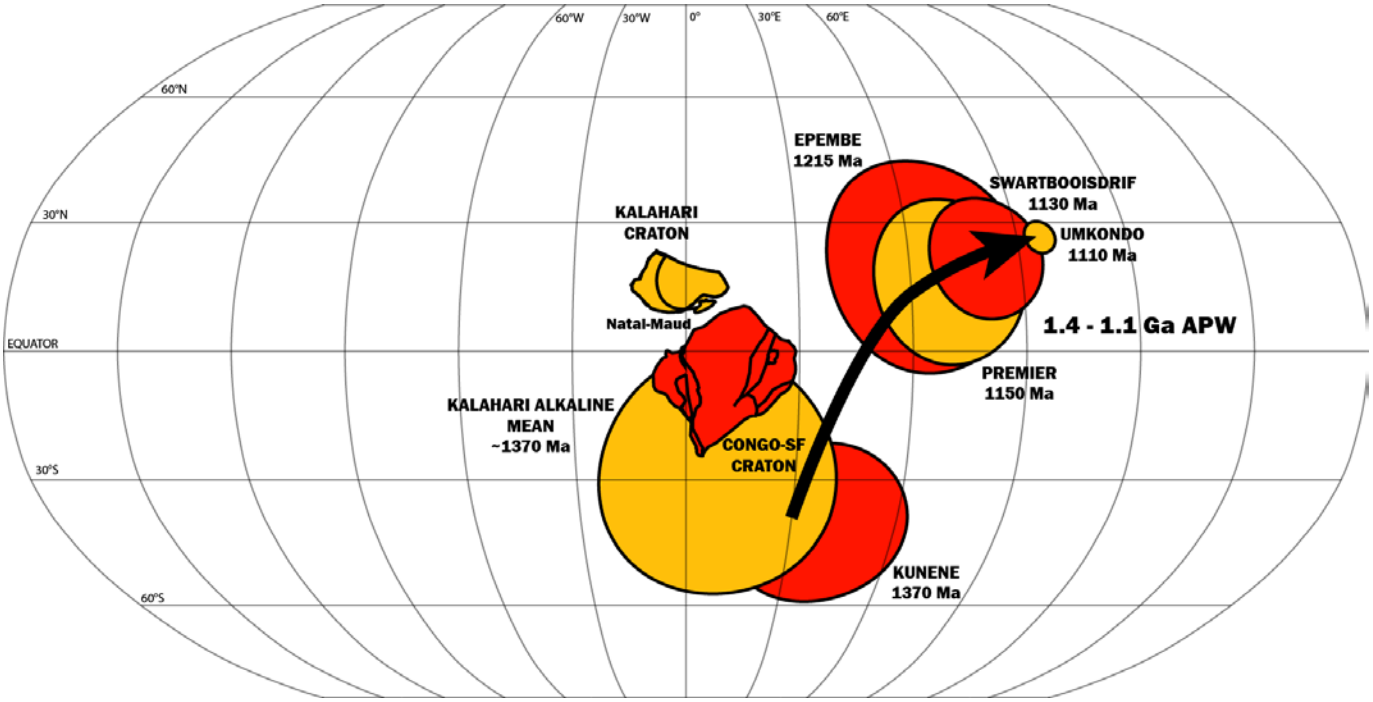

Figure 21: The "closest approach" hypothesis for the 1.2-1.1 Ga poles brings the Kalahari craton adjacent to the Congo-SF craton (Euler parameters: 08.9°N, 50.3°E, -69.8°), eliminating the possibility of a third craton between the two. All poles are still within error of each other, and the 1370 Ma poles also begin to overlap, demonstrating the possibility that this configuration was maintained into the middle Mesoproterozoic. However, orogenic development of the Natal-Maud orogeny at ~1.2 Ga finds no counterpart in the putatively adjacent Oubanguide margin of northern Congo; thus the model is challenged on tectonostratigraphic grounds.

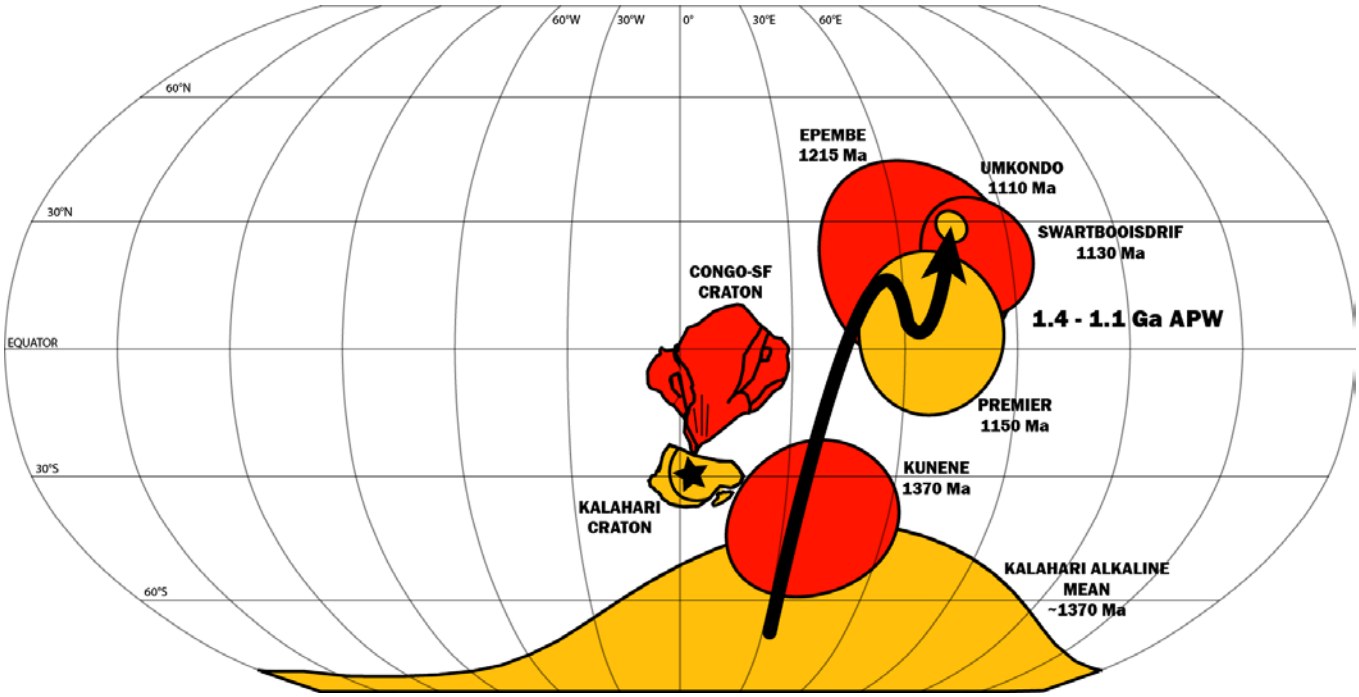

Figure 22: The final configuration we propose optimizes the geological correlations between the two cratons. With the Kalahari craton in this position, Umkondo magmatism (marked with a star) can be linked as a source for dykes (marked with lines) of the same age in the Congo-SF. However, this rotation (Euler parameters: 15.6°S, 13.7°E, -46.1°) is barely permitted in terms of correlating paleopoles from the two cratons.

CONCLUSIONS AND SUGGESTIONS FOR FURTHER WORK

Based on our three new preliminary paleomagnetic poles from Mesoproterozoic igneous suites in the southernmost Congo craton, we are able to address issues involving the relative positions of Congo and Kalahari prior to the Pan-African orogenic cycle. First, we suggest a configuration which optimizes the apparent polar wander (APW) path for the two cratons. In this model, the Kalahari and Congo-SF cratons are on the same plate, but located about 30° apart, suggesting that a "mystery" craton may have existed between the two and is either undiscovered or has been subsequently destroyed. The next model we propose brings the Kalahari craton closer to the Congo-SF craton. We disprove the null hypothesis that the two cratons could have been connected in their modern-day configuration, and then provide a model where the Kalahari craton is connected to Congo-SF in the north. Geologically, there is little evidence in support of this configuration, making it less optimal than the first. Finally, we suggest a third model using an integrative approach, optimizing the geological evidence on both cratons while keeping paleopoles within error of each other. This configuration allows for the connection between the Umkondo large igneous province and subsequent dyke intrusions in Congo-SF, but does not optimize the APW path as in our first model. Although only two pairs of paleopoles are used as constraints in making these models, we include our preliminary Kunene Anorthosite Complex paleopole and a comparable Kalahari Alkaline Mean paleopole in each figure for comparison. In the second and third models, these poles overlap within error, suggesting that the two cratons could have been connected earlier than 1215 Ma. However, due to the low number of samples in our Kunene paleopole and the high error on the Kalahari Alkaline Mean paleopole, these comparisons do not hold significant weight.

In order to verify the results presented in this thesis, further sampling of all three units should be completed. With more data, the range of error for each one of these preliminary paleopoles may be greatly reduced, allowing for a more complete paleomagnetic record of the Congo-SF craton through the Mesoproterozoic. This work, then, should be developed further by linking these Mesoproterozoic poles with the Neoproterozoic poles we have calculated (including the Sanyika Redbeds of Tanzania) to create an extended APW path for the craton, demonstrating craton movement through Nuna breakup to terminal Proterozoic-Cambrian Gondwana assembly. More locally, supplementing these paleopoles with more data will provide further insight into the characteristics and closure of an ocean between Kalahari and Congo-SF, as well as the subsequent orogeny of the Damara belt through central Namibia.

ACKNOWLEDGEMENTS

Lab work in 2013 was funded by David Evans' discretionary research accounts provided by Yale University. Field work and lab work in 2014 were funded by the Karen Von Damm '77 Undergraduate Research Fellowship in Geology & Geophysics. A Morse College Mellon Undergraduate Research Grant covered transportation costs for the presentation of this research at the 2015 American Geophysical Union-Geological Association of Canada Joint meeting in Montreal.

Personally, I cannot thank my adviser, David Evans, enough for his guidance and support throughout my undergraduate career. I also thank Richard Hanson of Texas Christian University for lending his insight and sacrificing his ankle during the summer 2014 field season, XinXin Xu for being an amazing field assistant while keeping both sass and morale high at all times, and Johanna Salminen of the University of Helsinki for (sometimes literally) carrying the team through the field. In addition, a sincere thank you goes out to Charlie Hoffmann, who helped coordinate logistics with the Geological Survey of Namibia, and the Miller family of Farm Aruab for graciously opening their home to us.

REFERENCES

Butler, Robert F, 1992. *Paleomagnetism: Magnetic Domains to Geologic Terranes*. Blackwell Scientific Publications, Electronic Edition (September 2004), Web: http://www.geo.arizona.edu/Paleomag/book/.

Doppelhammer, Sheila K. and R. B. Hargraves, 1994. "Paleomagnetism of the Schuller and Franspoort kimberlite pipes in South Africa and an improved Premier pole." *Precambrian Research* 69.1-4, 193-197.

Drüppel, K., Brandt, S., and Okrusch, M., 2000, "Evolution of the anorthositic Kunene intrusive complex and the metamorphic rocks of the Epupa complex, NW Namibia: Evidence for co-genetic formation during Proterozoic crustal extension?": GeoLuanda 2000 conference, Luanda, Angola, May 21–24, 47–48.

Drüppel, Kirsten, Jochen Hoefs, and Martin Okrusch, 2005. "Fenitizing Processes Induced by Ferrocarbonatite Magmatism at Swartbooisdrif, NW Namibia." *Journal of Petrology* 46.2, 377-406.

Ernst, Richard E., et al., 2013. "Mesoproterozoic intraplate magmatic 'barcode' record of the Angola portion of the Congo Craton: Newly dated magmatic events at 1505 and 1110 Ma and implications for Nuna (Columbia) supercontinent reconstructions." *Precambrian Research* 230, 103-118.

Evans, David A. D., 2013. "Reconstructing pre-Pangean supercontinents." *Geological Society of America Bulletin* 125, 1735-1751.

Evans, David A. D., 2003. "True polar wander and supercontinents." *Tectonophysics* 362, 303-320.

Evans, David A.D., et al., in press. "Return to Rodinia? Moderate to high paleolatitude of the São Francisco/Congo craton at 925 Ma." *Geological Society of London, Special Publication 424*.

Evans, David A. D., and Ross N. Mitchell, 2011. "Assembly and breakup of the core of Paleoproterozoic-Mesoproterozoic supercontinent Nuna." *Geology* 39, 443-446.

Ferguson, J., McIver J. R., and Danchlin, R. V., 1975. "Fenitisation associated with the alkaline-carbonatite complex of Epembe, South West Africa." *Trans. Geol. Soc. S. Afr.* 78: 111-121.

Fisher, R. 1953. Dispersion on a sphere. *Proceedings of the Royal Society of London. Series A*, 219, 295–305.

Fisher, N. I., T. Lewis, and B. J. J. Embleton, 1987. *Statistical Analysis of Spherical Data*. Cambridge University Press, Cambridge.

Gose, W. A., et al., 2006. "Paleomagnetism of the 1.1 Ga Umkondo large igneous province in southern Africa." *Journal of Geophysical Research* 111:B9, 2156-2202.

Gose, W. A., et al., 2013. "Reconnaissance paleomagnetic studies of Mesoproterozoic alkaline igneous complexes in the Kaapvaal craton, South Africa." *Journal of African Earth Sciences* 85, 22-30.

Gray, David R, et al., 2006. "$^{40}Ar/^{39}Ar$ Thermochronology of the Pan-African Damara Orogen, Namibia, with implications for tectonothermal and geodynamic evolution." *Precambrian Research* 150.1-2, 49-72.

Grunow, Anne, Richard Hanson, and Terry Wilson, 1996. "Were aspects of Pan-African deformation linked to Iapetus opening?" *Geology* 24, 1063-1066.

Hanson, Richard E., 2003..*Geological Society of London Special Publication*.

Hedberg, R. M., 1979. *Stratigraphy of the Ovamboland Basin, South West Africa*. Bulletin of the Precambrian Research Unit, University of Cape Town, v. 24, 325 pp.

Hoffman, P. F. and Halverson, G.P., 2008. "Otavi Group of the western Northern Platform, the Eastern Kaoko Zone and the western Northern Margin Zone." *The Geology of Namibia*, Vol. 2 (Ed. R.Mc.G. Miller), Geol. Surv. Namibia, Windhoek.

Hoffman, P. F., 2011. "Strange bedfellows: glacial diamictite and cap carbonate from the Marinoan (635 Ma) glaciation in Namibia." *Sedimentology* 58, 57-119.

Jones, Craig H., 2002. "User-driven integrated software lives: "Paleomag" paleomagnetics analysis on the Macintosh." *Computers & Geosciences* 28, 1145-1151.

Kirschvink, J. L., 1980. "The least-squares line and plane and the analysis of paleomagnetic data." *Geophys. J. R. Soc.* 62, 699-718.

Li, Z. X., et al., 2008. "Assembly, configuration, and break-up history of Rodinia: A synthesis." *Precambrian Research* 160, 179-210.

Littmann, S., Romer R. I, and Okrusch M., 2000. "Nephelinsyenite der Epembe-Swartbooisdrif-Alkali-Provinz (ESAP)/NW Namibia." *Berichte der Deutschen Mineralogischen Gesellschaft, Beihefte zum European Journal of Mineralogy* 12, 115.

Maier, W. D., et al., 2013. "The Kunene Anorthosite Complex, Namibia, and Its Satellite Intrusions: Geochemistry, Geochronology, and Economic Potential." *Economic Geology* 108, 953-986.

Menge, G. F. W., 1986. "Sodalite-carbonatite deposits of Swartbooisdrif, South West Africa/Namibia." *Mineral deposits of southern Africa: Geol. Soc. S. Afr*., 2261-2268.

Menge, G. F. W., 1996. "The eastern portion of the Kunene complex, its satellite intrusions and the alkaline suite between Epembe and Swartbooisdrif." Unpublished monograph.

Meert, Joseph G., Rob van der Voo, and Samwel Ayub, 1995. "Paleomagnetic investigation of the Neoproterozoic Gagwe lavas and Mbozi complex, Tanzania and the assembly of Gondwana." *Precambrian Research* 74, 225-244.

Miller, R. McG., 2008. "Epembe—Swartbooisdrif Alkaline Suite." *The Geology of Namibia.* Volume 1: Archean to Mesoproterozoic, 10-1 – 10-8.

Mitchell, Ross N., David A. D. Evans and Taylor M. Kilian, 2010. "Rapid Early Cambrian rotation of Gondwana." *Geology* 38.8, 755-758.

Pesonen, L. J., et al., 2003. "Paleomagnetic configuration of continents during the Proterozoic." *Tectonophysics* 375, 289-324.

Piper, J. D. A., 1974. "Magnetic Properties of the Cunene Anorthosite Complex, Angola." *Physics of the Earth and Planetary Interiors* 9, 353-363.

Piper, J. D. A., 1972. "A Palaeomagnetic Study of the Bukoban System, Tanzania." *Geophysical Journal International* 28.2, 111-127.

Prave, Anthony R., 1996. "Tale of three cratons: Tectonostratigraphic anatomy of the Damara orogen in northwestern Namibia and the assembly of Gondwana." *Geology* 24, 1115-1118.

Schreiber, U.M., 2002, compiler. Sheet 1712 - Swartbooisdrif. Geological Map of Namibia, 1:250,000 Geological Series. Geological Survey of Namibia, Windhoek.

Seth, Barbara, et al., 2003. "Mesoproterozoic U-Pb and Pb-Pb ages of granulites in NW Namibia: reconstructing a complete orogenic cycle." *Precambrian Research* 126, 147-168.

Simpson, E.S.W., 1970. "The anorthosite of southern Angola: a review of present data," *African Magmatism and Tectonics*, Oliver and Boyd: Edinburgh, 89-96.

Torsvik, Trond H., 2012. "Phanerozoic polar wander, paleogeography and dynamics." *Earth Science Reviews* 114, 325-368.

Van der Voo, R., 1990. "The reliability of paleomagnetic data." Tectonophysics 184, 1–9.

von Seckendorff, V., Drüppel, K., Okrusch, M., Cook, N.J., and Littmann, S., 2000. "Oxide-sulphide relationships in sodalite-bearing metasomatites of the Epembe-Swartbooisdrif Alkaline Province, north-west Namibia." *Mineralium Deposita* 35, 430-450.

Vissers, R. L. M. and P. Th. Meijer, 2012. "Mesozoic rotation of Iberia: Subduction in the Pyrenees?" *Earth Science Reviews* 110, 93-110.

Weil, Arlo B., et al., 1998. "The Proterozoic supercontinent Rodinia: paleomagnetically derived reconstructions for 1100 to 800 Ma." *Earth and Planetary Science Letters* 154, 13-24.

Williams, Simon E., et al., 2012. "An open-source software environment for visualizing and refining plate tectonic reconstructions using high-resolution geological and geophysical data sets." *GSA Today* 22.4/5, 4-9.

Wu, Fu-Yuan, et al., 2013. "In situ U-Pb age determination and Sr-Nd isotopic analysis of perovskite from the Premier (Cullinan) Kimberlite, South Africa." *Chemical Geology* 353, 83-95.

APPENDIX